Neurobiology of Disease 145 (2020) 105043

Contents lists available at ScienceDirect

Neurobiology of Disease

journal homepage: www.elsevier.com/locate/ynbdi

# Impairment of adenosinergic system in Rett syndrome: Novel therapeutic target to boost BDNF signalling

Catarina Miranda-Lourenço[a,1], Sofia T. Duarte[a,b,1], Cátia Palminha[a], Cláudia Gaspar[c], Tiago M. Rodrigues[a,d], Teresa Magalhães-Cardoso[e], Nádia Rei[a], Mariana Colino-Oliveira[a], Rui Gomes[c], Sara Ferreira[c], Jéssica Rosa[a], Sara Xapelli[a], Judith Armstrong[f], Àngels García-Cazorla[g], Paulo Correia-de-Sá[e], Ana M. Sebastião[a,1], Maria José Diógenes[a,1,*]

[a] Instituto de Farmacologia e Neurociências, Faculdade de Medicina e Instituto de Medicina Molecular – João Lobo Antunes, Universidade de Lisboa, Lisboa, Portugal
[b] Child Neurology Department, Hospital Dona Estefânia - Centro Hospitalar Universitário de Lisboa Central, Portugal
[c] Instituto de Medicina Molecular – João Lobo Antunes, Universidade de Lisboa, Lisboa, Portugal
[d] Institute of Molecular and Clinical Ophtalmology, Mittlere Strasse 91, CH-4031 Basel, Switzerland
[e] Laboratório de Farmacologia e Neurobiologia / MedInUP, Instituto de Ciências Biomédicas Abel Salazar – Universidade do Porto (ICBAS-UP), Porto, Portugal
[f] Genetics Department, Hospital Sant Joan de Deu. Institut Pediàtric de Recerca and CIBERER. (ISCIII), Barcelona, Spain
[g] Synaptic Metabolism Laboratory, Neurology Department; Institut Pediàtric de Recerca and CIBERER. (ISCIII), Barcelona, Spain

ARTICLE INFO

*Keywords:*
Rett syndrome
Brain-derived neurotrophic factor
TrkB receptors
Adenosinergic system
*Mecp2 knockout* model

ABSTRACT

Rett syndrome (RTT; OMIM#312750) is mainly caused by mutations in the X-linked *MECP2* gene (methyl-CpG-binding protein 2 gene; OMIM*300005), which leads to impairments in the brain-derived neurotrophic factor (BDNF) signalling. The boost of BDNF mediated effects would be a significant breakthrough but it has been hampered by the difficulty to administer BDNF to the central nervous system. Adenosine, an endogenous neuromodulator, may accomplish that role since through $A_{2A}R$ it potentiates BDNF synaptic actions in healthy animals. We thus characterized several hallmarks of the adenosinergic and BDNF signalling in RTT and explored whether $A_{2A}R$ activation could boost BDNF actions.

For this study, the RTT animal model, the *Mecp2 knockout* (*Mecp2*$^{-/y}$) (B6.129P2 (C)-Mecp2tm1.1Bird/J) mouse was used. Whenever possible, parallel data was also obtained from *post-mortem* brain samples from one RTT patient. *Ex vivo* extracellular recordings of field excitatory post-synaptic potentials in CA1 hippocampal area were performed to evaluate synaptic transmission and long-term potentiation (LTP). RT-PCR was used to assess mRNA levels and Western Blot or radioligand binding assays were performed to evaluate protein levels. Changes in cortical and hippocampal adenosine content were assessed by liquid chromatography with diode array detection (LC/DAD).

Hippocampal *ex vivo* experiments revealed that the facilitatory actions of BDNF upon LTP is absent in *Mecp2*$^{-/y}$ mice and that TrkB full-length (TrkB-FL) receptor levels are significantly decreased. Extracts of the hippocampus and cortex of *Mecp2*$^{-/y}$ mice revealed less adenosine amount as well as less $A_{2A}R$ protein levels when compared to WT littermates, which may partially explain the deficits in adenosinergic tonus in these

*Abbreviations:* [$^3$H]DPCPX, 1,3-[3H]-dipropyl-8-cyclopentylxanthine; DPCPX, 1,3-dipropyl-8-cyclopentylxanthine; 5-ITU, 5-iodotubercidin; $A_1R$, $A_1$ receptors; $A_{2A}R$, $A_{2A}$ receptors; BDNF, brain-derived neurotrophic factor; aCSF, cold artificial cerebrospinal fluid; fEPSPs, Field excitatory postsynaptic potentials; I/O, Input–output curve; LTP, long-term potentiation; Mecp2$^{-/y}$, MECP2 knockout; MECP2, methyl-CpG binding protein 2; CPA, N6-Cyclopentyladenosine; PVDF, polyvinylidene fluoride; qPCR, quantitative PCR; RIPA, Radio-Immunoprecipitation Assay; RTT, Rett Syndrome; SDS-PAGE, sodium dodecyl sulphate-polyacrylamide gel electrophoresis; TrkB-FL, Tropomyosin receptor kinase B full-length (TrkB-FL); WT, wild type

* Corresponding author.
*E-mail addresses:* catarinalourenco@medicina.ulisboa.pt (C. Miranda-Lourenço), Sofia.duarte22@hotmail.com (S.T. Duarte), catiapalminha@gmail.com (C. Palminha), cscgaspar@gmail.com (C. Gaspar), tiago.fm.rod@gmail.com (T.M. Rodrigues), tmcardoso@icbas.up.pt (T. Magalhães-Cardoso), nadia.rei@gmail.com (N. Rei), Mcolino.oliveira@gmail.com (M. Colino-Oliveira), ragomes@medicina.ulisboa.pt (R. Gomes), ssgferreira@gmail.com (S. Ferreira), jessicarosa@campus.ul.pt (J. Rosa), sxapelli@medicina.ulisboa.pt (S. Xapelli), jarmstrong@sjdhospitalbarcelona.org (J. Armstrong), agarcia@sjdhospitalbarcelona.org (À. García-Cazorla), farmacol@icbas.up.pt (P. Correia-de-Sá), anaseb@medicina.ulisboa.pt (A.M. Sebastião), diogenes@medicina.ulisboa.pt (M.J. Diógenes).
[1] Equal contribution.
Full Address: Edifício Egas Moniz, Av. Professor Egas Moniz, 1649–028 Lisbon, Portugal.

https://doi.org/10.1016/j.nbd.2020.105043
Received 21 April 2020; Received in revised form 23 July 2020; Accepted 8 August 2020
Available online 14 August 2020

animals. Remarkably, the lack of BDNF effect on hippocampal LTP in *Mecp2*$^{-/y}$ mice was overcome by selective activation of $A_{2A}R$ with CGS21680.

Overall, in *Mecp2*$^{-/y}$ mice there is an impairment on adenosinergic system and BDNF signalling. These findings set the stage for adenosine-based pharmacological therapeutic strategies for RTT, highlighting $A_{2A}R$ as a therapeutic target in this devastating pathology.

## 1. Introduction

Rett Syndrome (RTT) is a progressive genetic neurodevelopmental disorder characterized by cognitive and motor impairments, development of stereotypic hand movements and epilepsy. A developmental regression with loss of skills acquired during an apparently normal period after birth (*ca.* 6 months) is typical (Neul et al., 2014). RTT affects 1:10.000 female live births worldwide and it is the main genetic cause of intellectual disability in girls (Chahrour and Zoghbi, 2007). About 90% of RTT cases are caused by mutations in methyl-CpG binding protein 2 gene (*MECP2*), located on the X chromosome, responsible for encoding the MeCP2 protein (Amir et al., 1999; Liyanage and Rastegar, 2014). This protein is an essential epigenetic factor that regulates the expression of several genes (Bedogni et al., 2014; Lewis et al., 1992; Liyanage and Rastegar, 2014). One of the genes under the jurisdiction of MeCP2 is the brain-derived neurotrophic factor (BDNF) gene, which encodes the neurotrophin BDNF (Li and Pozzo-Miller, 2014). BDNF plays essential functions during neuronal development and maturation, including axonal targeting, dendritic growth, synaptic maturation and it is also a modulator of synaptic plasticity (Binder and Scharfman, 2004). Its actions are mediated by the high-affinity Tropomyosin receptor kinase B full-length (TrkB-FL) receptors. BDNF binding to TrkB-FL receptors induces receptor dimerization and kinase domain transactivation, subsequently leading to activation of specific signalling transduction pathways (Huang and Reichardt, 2003). BDNF also has affinity to TrkB truncated isoforms (TrkB-Tc), which act as negative effectors of full-length receptors through their own pathways (Eide, 1996; Rose et al., 2003).

Previous studies have shown that BDNF levels are decreased in RTT mouse models; thus, deregulation of BDNF functions in RTT has been suggested as a disease mechanism for the deficits in synaptic transmission and plasticity, neuronal survival and development (Asaka et al., 2006; Deng et al., 2007; Li et al., 2012; Li and Pozzo-Miller, 2014; Moretti et al., 2006; Robinson et al., 2012). Accordingly, BDNF mRNA levels were shown to be decreased in *post-mortem* brain samples from human patients (Abuhatzira et al., 2007). However, no changes were detected in BDNF protein levels on cerebrospinal fluid and blood serum samples (Riikonen, 2003; Vanhala et al., 1998). Experiments where BDNF expression levels were genetically manipulated in RTT mouse models have shown that BDNF overexpression led to symptomatic improvements (Chen et al., 2007; Guy et al., 2007, for review see Li and Pozzo-Miller, 2014). However, therapeutic designs involving BDNF delivery to the brain are still inefficient, given BDNF's inability to cross the blood-brain barrier (Poduslo and Curran, 1996). In order to overcome this limitation, novel strategies should be considered, including the use of small molecules able to boost BDNF actions.

It is now currently accepted that most BDNF actions are dependent on the activation of a specific type of adenosine receptors, the $A_{2A}$ receptors ($A_{2A}R$) (Sebastião et al., 2011). On the other hand, another subtype of adenosine receptor, the $A_1R$, has well known inhibitory actions upon synaptic transmission with impact in epilepsy control (Rombo et al., 2014). Modulation of adenosine receptors, mostly $A_1$ and $A_{2A}R$ has long been considered as a useful strategy to treat several neurologic disorders, such as sleep disorders, epilepsy and neurodegenerative diseases (Sebastião and Ribeiro, 2009), but has never been tested in RTT. Modulators of adenosine receptors were already tested in clinical trials for treatment of other diseases (Chen et al., 2007). In light of the knowledge on: i) the cross-talk between BDNF and adenosine receptors, ii) the advantages of potentiating BDNF actions in RTT, and iii) the deregulation of the adenosinergic system in several pathological conditions co-occurring with epilepsy, we hypothesized that adenosine receptors could be therapeutic targets in RTT. To tackle this hypothesis, we used a well-recognized RTT mice model, the *Mecp2 knockout* (*Mecp2*$^{-/y}$), to identify putative changes in the adenosinergic system and to assess whether pharmacological modulation of adenosine receptors could potentiate BDNF effects in this RTT model.

## 2. Materials and methods

### 2.1. Animals

Experiments were performed in a mouse model of RTT (B6.129P2)C)-Mecp2$^{tm1.1Bird}$/J [*MECP2* knockout; *Mecp2*$-^{/y}$], JAX #003890; (Guy et al., 2001) during the symptomatic stage (males between 6 and 10 weeks old; females between 26 and 28 weeks); wild type (WT) littermates were used as control. The genotype of animals was determined by PCR analysis, as previously described (Guy et al., 2007). The animals were housed on a 12 h light/dark cycle, with food and water provided *ad libitum*. Throughout the experimental work, care was taken to minimize the number of animals sacrificed. All animals were handled according to the Portuguese law on Animal Care and European Community guidelines (86/609/EEC). Mice were sacrificed by decapitation under deep isoflurane anaesthesia.

### 2.2. Post-mortem human brain sample

The brain tissue of one 11 year-old girl with RTT (MeCP2 mutation - R255X) who died after a severe pneumonia was dissected and different anatomic regions were immediately frozen at −80 °C. Age- and sex-matched cortical tissue was kindly provided by the "Biobank de Hospital Infantil Sant Joan de Déu (HSJD) per la Investigació" integrated in the "Spanish Biobank Network of ISCIII for the sample and the data procurement", to whom we are indebted.

### 2.3. Ex vivo electrophysiological recordings

After decapitation, the mouse brain was quickly removed, hemisected and both hippocampi were dissected free within ice-cold artificial cerebrospinal fluid (aCSF) solution: NaCl 124 mM; KCl 3 mM; $NaH_2PO_4$ 1.25 mM; $NaHCO_3$ 26 mM; $MgSO_4$ 1 mM; $CaCl_2$ 2 mM; and glucose 10 mM, previously gassed with 95% $O_2$ and 5% $CO_2$, pH 7.4. Slices (400 μm thick) were cut perpendicularly to the long axis of the hippocampus with a McIlwain tissue chopper and allowed to recover functionally and energetically for at least 1 h in a resting chamber, filled with aCSF, at room temperature. Slices were then transferred to a submerging chamber (1 ml) and continuously superfused at 3 ml/min with gassed aCSF at 32 °C; drugs were added to this superfusion solution. Field excitatory postsynaptic potentials (fEPSPs) were recorded extracellularly through a microelectrode (2–8 MΩ resistance, Harvard apparatus Ltd., Cambridge, MA, USA) placed in *stratum radiatum* of hippocampal CA1 area. One or two pathways (as indicated) of the Schaffer collateral/commissural fibers were stimulated (rectangular 0.1 ms pulses), every 15 s (for input-output [I/O] curves and basal synaptic transmission) or every 20 s (for long-term potentiation [LTP] recordings) through a bipolar concentric electrode placed on the Schaffer fibers, in *stratum radiatum* near CA3–CA1 border. The intensity

of stimulus (80–200 μA) was initially adjusted to obtain a large fEPSP slope with a minimum population spike contamination. The averages of 8 (for I/O curves and basal synaptic transmission) or 6 (for LTP recordings) consecutive responses were obtained and the slope of the initial phase of the potential was quantified. Recordings were obtained with an Axoclamp 2B amplifier (Axon Instruments, Foster City, CA, USA), digitized and continuously stored on a personal computer with the LTP software (Anderson and Collingridge, 2001).

#### 2.3.1. Basal synaptic transmission

Alteration in synaptic transmission induced by drugs was evaluated as the % change in the average slope of the fEPSP in relation to the average slope of the fEPSP measured during the 10 min that preceded the addition of drugs to the superfusion solution, as described previously (Diógenes et al., 2004).

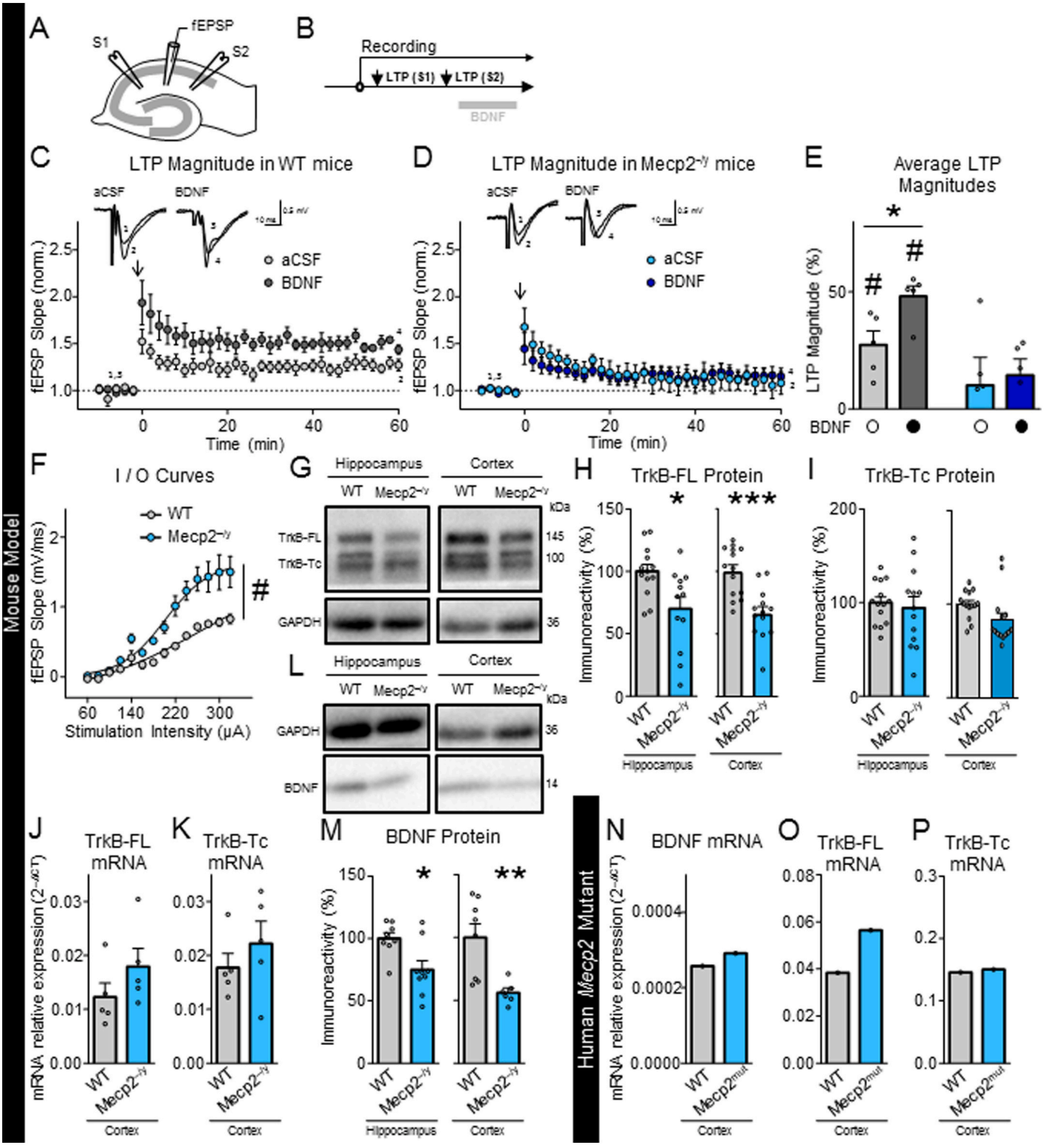


*(caption on next page)*

**Fig. 1.** BDNF loses the facilitatory effect upon LTP in Mecp2$^{-/y}$ animals: A shows schematic representation of a transverse hippocampal slice and the recording configuration used, as described in methods section. B represents the protocol used to evaluate the effect of BDNF upon LTP (see methods). Panels C and D show time courses of averaged changes in fEPSP slope induced by the θ-burst stimulation in the absence (light circles) or in the presence (dark circles) of BDNF in hippocampal slices taken from WT (grey symbols,n = 5) animals or from Mecp2$^{-/y}$ (blue symbols,n = 5) animals. Traces from representative experiments are shown for WT and Mecp2$^{-/y}$ animals. Histogram E depicts the magnitude of LTP in the absence (light bars) and the presence of BDNF (20 ng/ml, dark bars) in hippocampal slices from WT (grey) or Mecp2$^{-/y}$ animals (blue). F shows the input/output (I/O) curves corresponding to responses generated by various stimulation intensities (60–340 μA) in WT slices (grey circles,*n* = 4) and Mecp2$^{-/y}$ slices (blue circles,n = 4). *$p < 0.05$ (paired Student's *t*-test) as compared with absence of BDNF in the same experiments.
In H,I and M are shown the averaged of TrkB-FL($WT_{hip}$,n = 13;$WT_{ctx}$,n = 14;$Mecp2^{-/y}_{hip}$,n = 12;$Mecp2^{-/y}_{ctx}$,n = 13), TrkB-Tc ($WT_{hip}$, n = 14;$WT_{ctx}$,n = 14;$Mecp2^{-/y}_{hip}$,n = 13;$Mecp2^{-/y}_{ctx}$,n = 14) and BDNF($WT_{hip}$,n = 8;$WT_{ctx}$,n = 8;$Mecp2^{-/y}_{hip}$,n = 9;$Mecp2^{-/y}_{ctx}$,n = 6) density evaluated by Western-Blot analysis in hippocampal and cortical homogenates from WT(grey) and Mecp2$^{-/y}$(blue) animals with 6–10 weeks of age. G and L show representative bands obtained by Western Blot for each studied protein. All values presented are mean ± SEM and are represented in % of WT protein. J,K and N–P depicted data obtained by qPCR showing mRNA levels of TrkB-FL(J,O), TrkB-Tc(K,P) and BDNF(N) in cortical samples from WT(light bar,n = 5) and Mecp2$^{-/y}$(dark bar,n = 5) animals (J and K) and from a human temporal cortex sample (N,O and P) taken from a control patient (white bar,n = 1) and a RTT patient (black bar,n = 1). All values are mean ± standard error of mean (SEM). *p < 0.05; **p < 0.01; ***p < 0.001 (Student's t-test); #p < 0.05 (F test).

#### 2.3.2. LTP induction and quantification

*f*EPSPs were elicited and recorded as outlined above. Stimulation was delivered alternatively to two independent pathways (Fig. 1A). LTP was induced by a θ-burst protocol consisting of three trains of 100 Hz, three stimuli, separated by 200 ms as previously described (Diógenes et al., 2011). LTP was quantified as the % change in the average slope of the fEPSP taken from 50 to 60 min after LTP induction in relation to the average slope of the fEPSP measured during the 10 min that preceded the induction of LTP. In each individual experiment, the same LTP-inducing paradigm was delivered to each pathway. At 1 h after LTP induction in one of the pathways, BDNF (20 ng/ml) was added to the superfusion solution and LTP was induced in the second pathway, no less than 20 min after BDNF perfusion and only after stability of fEPSP slope values was observed for at least 10 min (Fig. 1B). The effect of BDNF upon LTP was evaluated by comparing the magnitude of LTP in the first pathway in the absence of BDNF (control pathway), with the magnitude of LTP in the second pathway in the presence of BDNF (test pathway); each pathway was used as control or test on alternate days. The same experimental protocol was used to test the effect of CGS21680, an $A_{2A}R$ agonist, on LTP magnitude. In order to test the modulatory effect of $A_{2A}R$ activation on BDNF effect upon LTP, CGS21680 was added 60 min after LTP induction in the first pathway and at least 20 min before BDNF were added to the superfusion bath. Thus, in these experiments, LTP was induced in the second pathway in the presence of both CGS21680 and BDNF. These drugs remained in bath until the end of the experiment.

#### 2.3.3. Input–output curve (I/O)

After obtaining a stable baseline for at least 10 min, the stimulus delivered to the slice was decreased until no fEPSP was evoked and subsequently increased in 20 μA steps. For each stimulation intensity, data from three consecutive averages of 8 fEPSP were collected. Inputs delivered to slices typically ranged from 60 μA to a supramaximal stimulation of 320 μA. The input–output curve was plotted as the relationship of fEPSP slope *vs* stimulus intensity, which provides a measure of synaptic efficiency as previously described (Diogenes et al., 2012).

### 2.4. Western Blot

Snap-frozen cortex and hippocampus samples from mice of each genotype (WT and *Mecp2*$^{-/y}$) were first disrupted with a Teflon pestle in Radio-Immunoprecipitation Assay (RIPA) buffer containing: 50 mM Tris-HCl (pH 7.5), 150 mM NaCl, 5 mM ethyl-enediamine tetra-acetic acid (EDTA), 0.1% SDS and 1%Triton X-100 and protease inhibitors cocktail (Mini-Complete EDTA-free; Roche Applied Science, Penzberg, Germany). All lysates were then vortexed and sonicated (3 cycles of 15 s), and clarified by centrifugation (13,000 *g*, 10 min). The protein content in the supernatant was determined by Bio-Rad DC reagent, a commercial Bradford assay (Sigma-Aldrich, St. Louis, MO, USA). Equal amount of protein was loaded (70 μg, except for $A_{2A}R$ blot: 200 μg) and separated on 10% sodium dodecyl sulphate-polyacrylamide gel electrophoresis (SDS-PAGE) and then transferred to polyvinylidene fluoride (PVDF) membrane (GE Healthcare, Buckinghamshire, UK). To check protein transfer efficiency, membranes were stained with Ponceau S solution. After blocking with a 5% non-fat dry milk solution in TBS-Tween (20 mM Tris base, 137 mM NaCl and 0.1% Tween-20), membranes were incubated with the primary antibody, diluted in 3% BSA solution in TBS-Tween (overnight at 4 °C) and then with secondary antibodies HRP-conjugated (1:10000, Santa Cruz Biotechnology, Dallas, TX, USA) diluted in blocking solution (1 h at room temperature). Immunoreactivity was visualized using ECL chemiluminescence detection system (Amersham-ECL Western Blotting Detection Reagents from GE Healthcare) and band intensities were quantified by digital densitometry (ImageJ 1.45 software). α-tubulin (1:3000, #ab4074, Abcam, Cambridge, MA, USA) or GAPDH (1:5000, #AM4300, Ambion by life technologies, Carlsbad, CA, USA) bands were used as loading control. The primary antibodies used were Anti-$A_{2A}R$ from Merk Millipore (1:1500, 05–717, Darmstadt, Germany) (Rei et al., 2020), Anti-$A_1R$ from Santa Cruz Biotecnology (1:1000, sc-28,995, Dallas, TX, USA), Anti-TrkB from BD Transduction Laboratories (1:1500, 610,101, Franklin Lakes, NJ, USA) and Anti-ADK from Bethyl Laboratories (1:1500, A304-280A, Montgomery, TX, USA).

### 2.5. Radioligand binding experiments

1,3-[3H]-dipropyl-8-cyclopentylxanthine ([$^3$H]DPCPX) binding studies were performed in cortical brain homogenates (40–80 μg protein per assay) of *Mecp2*$^{-/y}$ mice and WT littermates. [$^3$H]DPCPX binding was performed in an incubation solution (50 mM Tris-HCl buffer and 10 mM $MgCl_2$ (pH 7.4) and 4 U/ml ADA) for 120 min at room temperature, in a final volume of 200 μl. Specific binding was calculated by subtraction of the nonspecific binding, defined in the presence of 2 μM XAC. The reaction was stopped by addition of cold incubation buffer and vacuum filtration through glass fiber filters (FilterMAT for receptor binding, Skatron Instruments, Mountain View, CA, USA) using a semiautomatic cell harvester from Skatron Instruments. The samples were then transferred to scintillation vials and radioactivity was measured by a liquid scintillation analyser (Tri Carb 2900TR, Perkin-Elmer, IL). Membrane protein content was measured using the Bio-Rad DC reagent, a commercial Bradford assay (Berkeley, CA, USA).

### 2.6. RNA extraction and qPCR

Total RNA was extracted from cerebral cortex samples of *Mecp2*$^{-/y}$ mice, WT littermates and human samples using RNeasy Lipid Tissue Mini Kit (Qiagen, Venlo, Netherlands), according to the manufacturer's instructions. RNA concentration and purity were then evaluated by spectrophotometry based on optical density (OD) measurements at 260

and 280 mm (Model: NanoDrop-100; Thermo Scientific, Rockford, IL, USA). cDNA synthesis was performed in a 20 µl reaction mixture. 2 µg of total RNA were mixed with 1 µl random primer hexamers (Amersham Life Sciences, Buckinghamshire, UK) and 1 µl (each) of dATP, dTTP, dCTP and dGTP (10 mM). This mix was incubated 5 min at 65 °C and after cooling for 2 min on ice, the remaining reagents were added (4 µl of 25 mM $MgCl_2$, 2 µl of 10× RT buffer, 2 µl of 0.1 M DTT, 0.5 µl Superscript II Reverse Transcriptase (200 U); all reagents from Invitrogen, Life Technologies, Waltham, MA, USA). Parallel reactions for each RNA sample were run without Superscript II to evaluate the degree of genomic DNA contamination. Gene expression level was addressed by quantitative PCR (qPCR) using Power SYBR® Green Master Mix (Life Technologies, Waltham, MA, USA), and cDNA was used as template for the real-time PCR run in Rotor Gene 6000 (Corbett Life Science, Uithoom, Netherlands). Negative control PCR samples were run with no template. Relative mRNA expression was calculated using $2^{-\Delta ct}$ method and primers were previously optimized in order to establish annealing temperature and primer efficiency (e = 2 ± 0.2), calculated after serial primer dilutions and construction of respective standard curve (slope and $R^2$ respectively around −3.3 and 0.99; described in Schmittgen and Livak, 2008). Data were normalized to the expression of PPIA peptidylprolyl isomerase A (cyclophilin A) (CypA) and ribosomal protein L13A (Rpl13A) (Batalha et al., 2016). The 5′-3′ primer sequences used for Cyp A (125 bp) were TAT CTG CAC TGC CAA GAC TGA GTG (forward) and CTT CTT GCT GGT CTT GCC ATT CC (reverse); for Rpl13A (130 bp) were GGA TCC CTC CAC CCT ATG ACA (forward) and CTG GTA CTT CCA CCC GAC CTC (reverse); for $A_{2A}R$ (113 bp) were ATT CCA CTC CGG TAC AAT GG (forward) and AGT TGT TCC AGC CCA GCA T (reverse) (Batalha et al., 2016); for $A_1R$ (155 bp) were TCG GCT GGC TAC CAC CCC TTG (forward) and CCA GCA CCC AAG GTC ACA CCA AAG C (reverse); for TrkB-FL were GAG CTG CTG ACC AAC CTC CA (forward) and GTC CCC GTG CTT CAT GTA CTC A (reverse); for TrkB-T1 were TAA GAT CCC ACT GGA TGG GTA G (forward) and AAG CAG CAC TTC CTG GGA TA (reverse) (Karpova et al., 2014). Data acquisition was performed with Rotor-Gene Series Software 1.7 (Corbett Life Science) and data analysis was performed with Microsoft Excel, Office 2016, Redmond, WA, USA. For human brain cortex samples, the real time-PCR was run in 7500 Fast (Applied Biosystems, Foster City, CA, USA) and the normalization was done to GAPDH expression. Data acquisition was performed with 7500 software v2.0.6 (Applied Biosystems, Foster City, CA, USA) and data analysis was performed in Microsoft Excel, Office 2016, Redmond, WA, USA. The 5′-3′ primer sequences used for GAPDH were GGA GCT AAC GGA TTT GGT CG (forward) and GAC AAG CTT CCC GTT CTA G; for $A_{2A}R$ were AAC CTG CAG AAC GTC AC (forward) and GTC ACC AAG CCA TTG TAC CG (reverse) (Batalha et al., 2016); for $A_1R$ were GCC ACA GAC CTA CTT CCA CA (forward) and CCT TCT CGA ACT CGC ACT TG (reverse); for TrkB-FL were GGC CCA GAT GCT GTC ATT AT (forward) and TTC TGC TCA GGA CAG AGG TT (reverse) (Nicolini et al., 2015); for TrkB-T1 were TCT ATG CTG TGG TGG TGA TTG (forward) and GAG TCC AGC TTA CAT GGC AG (reverse) (Luberg et al., 2010).

### 2.7. Extraction and analysis of purines by liquid chromatography with diode array detection (LC/DAD)

The purines (ATP, AMP, adenosine and inosine) content of extracts from the cortex and hippocampus of WT and *Mecp2*$^{-/y}$ mice was measured by liquid chromatography with diode array detection (LC/DAD). Snap-frozen cortex and hippocampal tissue samples were stored at −80 °C until use. For extraction, the samples were defrosted (250 µl) in round-bottom microcentrifuge tubes followed by thorough tissue homogenization using a mixture of ice-cold acetonitrile: methanol: water (1:2:2) solution (Jackson et al., 2017) containing 2-chloro-adenosine (5 µM) as internal standard; the obtained mixture was centrifuged at 16000 *g* for 20 min at 4 °C. Tissue homogenization and centrifugation were repeated twice. The two recovered supernatant extracts (~250 µl each) were mixed together and, then, centrifuged again at 16000 *g* (for 20 min at 4 °C) using a 50-kDa cutoff filter (Amicon Ultra-0.5 50 K Filter Device; Merck KGaA, Darmstadt, Germany). After filtration, supernatant extracts were divided in 15-µl aliquots and stored at −80 °C until analysis. Using this procedure, recovery of adenine nucleosides was higher than 95%, as determined by adding 2-chloro-adenosine (5 µM) as internal standard before extraction.

Extraction media containing purines were 1/10 diluted with water before LC/DAD analysis. Chromatographic separation of nucleosides was carried out using an elution gradient composed of ammonium acetate (5 mM, with a pH of 6 adjusted with acetic acid) and methanol (Silva et al., 2020, 2017; Vieira et al., 2017). Separation of adenine nucleotides was carried using a paired-ion chromatography reagent (PIC Reagent A; Waters Chromatography Europe BV, Etten-Leur, The Netherlands) containing tetrabutylamonium phosphate (1 mM) in $KH_2PO_4$ (100 mM, at pH = 6) (Waters) and methanol. Separation of adenine nucleotides and nucleosides using both elution systems was achieved by reversed–phase liquid chromatography through a Hypersil GOLD C18 column (5 µM, 2.1 mm × 150 mm) equipped with a guard column (5 µm, 2.1 mm × 1 mm) and assayed using a Finigan Thermo Fisher Scientific System LC/DAD, equipped with an Accela Pump coupled to an Accela Autosample, a diode array detector and an Accela PDA running the X-Calibur software chromatography manager. Quantification of adenine nucleotides and nucleosides was carried out using calibration curves made of high-purity external standards, namely ATP, AMP, adenosine and inosine.

### 2.8. Drugs

BDNF was generously provided by Regeneron Pharmaceuticals; 2-[p-(2-carboxyethyl)phenethylamino]-50-N-ethylcarboxamido adenosine (CGS21680) was purchased from Sigma; N6-Cyclopentyladenosine (CPA) and 1,3-Dipropyl-8-cyclopentylxanthine (DPCPX) were purchased from Tocris Bioscience (Ballwin, MO, USA); 1[$^3$H]DPCPX was purchased from American Radiolabeled Chemicals, Inc.; ATP, AMP, adenosine, inosine, 2-chloro-adenosine and 5-iodotubercidin (ITU) were purchased from Sigma (St. Louis, MO, USA). BDNF was supplied in a 1.0 mg/ml stock solution in 150 mM NaCl, 10 mM sodium phosphate buffer, and 0.004% Tween 20. CGS21680, CPA and DPCPX were made up in 5 mM and ITU in 50 mM stock solutions in DMSO. [$^3$H] DPCPX was purchased as a 36.5 µM solution in ethanol. The maximum DMSO concentration (0.02%) applied to the preparations was devoid of action on fEPSPs (Tsvyetlynska et al., n.d.). Aliquots of the stock solutions were kept frozen at −20 °C until use.

### 2.9. Data analysis

The data are expressed as mean ± SEM of the n number of independent experiments. The significance of differences between the means of 2 conditions was evaluated by paired or unpaired *t*-tests; Welch correction was used in unpaired t-test as appropriate. Nonlinear regressions were used to fit data pertaining I/O curves and radioligand binding experiments. Values of $p < 0.05$ were considered to represent statistically significant differences. GraphPad Prism 5.00 was used to performed statistical analysis.

## 3. Results

### 3.1. BDNF does not increase the magnitude of LTP in the hippocampus of *Mecp2*$^{-/y}$ mice

LTP is generally regarded as the neurophysiological correlate for learning and memory and BDNF has a well-documented ability to increase its magnitude on hippocampal CA1 area through TrkB-FL receptors activation (Figurov et al., 1996; Minichiello et al., 1999). To

assess the functional impact of the decrease in BDNF levels in RTT (Li and Pozzo-Miller, 2014), we evaluated the effect of exogenously applied BDNF (20 ng/ml) upon LTP. As expected (Diógenes et al., 2011; Fontinha et al., 2008), the θ-burst paradigm applied to hippocampal slices, taken from wild type (WT) animals induced a robust LTP in the presence of BDNF (48.2 ± 4.5%, $n = 5$; Fig. 1C;E), which was significantly higher than the obtained in the absence of BDNF (27.5 ± 5.8%, n = 5; $p = 0.02$, paired *t*-test; Fig. 1C;E). Importantly, in the absence of BDNF, θ-burst stimulation induced a small, yet significant LTP in WT mice ($p = 0.009$, paired *t*-test), but not in *Mecp2*$^{-/y}$ mice ($p = 0.45$, paired t-test). Moreover, BDNF (20 ng/ml) did not further increase LTP magnitude in hippocampal slices taken from

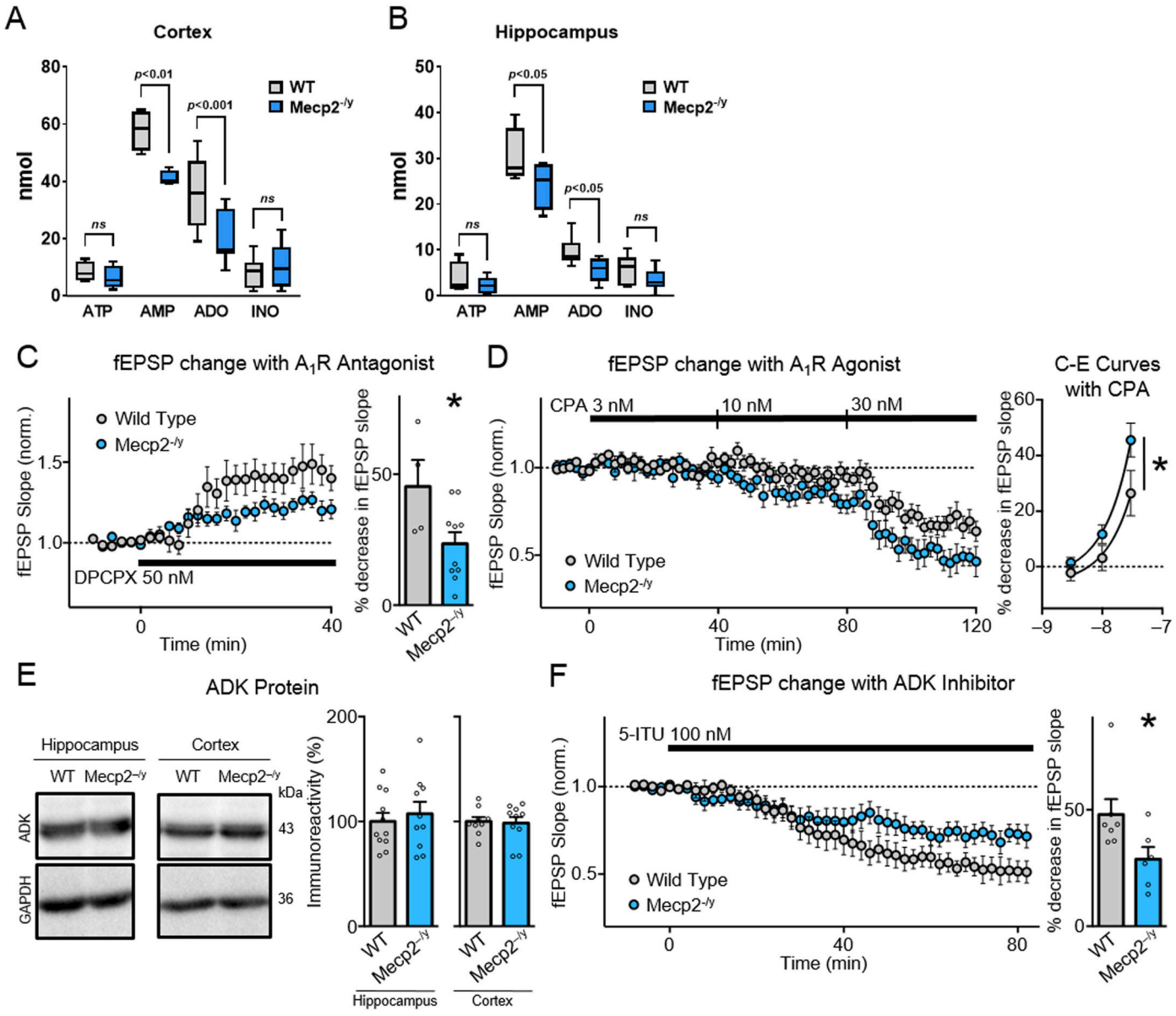


**Fig. 2.** Extracellular levels of adenosine are decreased in Mecp2$^{-/y}$ mice. In fig. A and B the ordinates represent the amount of ATP, AMP, adenosine (ADO) and inosine (INO) in nmol extracted from the cortex and hippocampus, respectively, of WT (grey bars) and Mecp2$^{-/y}$ (blue bars) mice and detected by LC/DAD (for details, see Materials and Methods). Represented are box-and-whiskers plots, with whiskers ranging from minimum to maximum values; horizontal lines inside boxes indicate the corresponding medians. Each data point represents four to eight individuals (see text for details); duplicate measurements were performed for each individual experiment. $p < 0.05$ (one-way ANOVA; uncorrected Fisher's LSD, with a single pooled variance) represent significant differences when compared to WT animals. The left panel of C shows the averaged time courses of changes in fEPSP slope induced by application of DPCPX (50 nM) in slices taken from WT (grey circles, $n = 4$) and Mecp2$^{-/y}$ (blue circles,n = 10) animals. The histogram on the right represent the averaged normalized decrease in fEPSPs slope in each animal group in response to DPCPX. D left panel shows the averaged time courses of changes in fEPSP slope induced by application of three different concentrations of CPA (3 nM, 10 nM, 30 nM) in slices taken from WT (grey circles,n = 7) and Mecp2$^{-/y}$ (blue circles,n = 7) animals. The right panel shows the comparison of the averaged effects of different concentrations of CPA in the different genotypes. Left panel of F shows the averaged time course of changes in fEPSP slope induced by ITU (100 nM) applied for 84 min. Hippocampal slices were taken from WT (grey circles,n = 7) and Mecp2$^{-/y}$ mice (blue circles, $n = 6$). The right panel shows the comparison of the averaged effects of ITU in the different genotypes. Left panel in E shows representative bands obtained by Western Blot of cortical and hippocampal tissue homogenates from Mecp2$^{-/y}$ and WT mice with 6–10 weeks of age. On the left panel, the histograms represent average band intensity for ADK obtained in samples from WT (grey bars,$n_{hip} = 11$; $n_{ctx} = 10$) and Mecp2$^{-/y}$ (blue bars,$n_{hip} = 9$; $n_{ctx} = 10$) hippocampal and cortical homogenates. All values presented are mean ± SEM and are represented in % of WT protein. *p < 0.05 (Student's *t*-test). (For interpretation of the references to colour in this figure legend, the reader is referred to the web version of this article.)

*Mecp2*$^{-/y}$ animals ($LTP_{CTR}$ = 10.2 ± 11.9%, $LTP_{BDNF}$ 14.5 ± 7.0%, n = 5; $p$ = 0.72, paired t-test; Fig. 1D;E).

To evaluate whether the impairment of LTP in *Mecp2*$^{-/y}$ animals could be due to changes in baseline synaptic efficiency, I/O curves were performed. Hippocampal slices taken from *Mecp2*$^{-/y}$ animals displayed higher $E_{max}$ values when compared with WT animals ($Emax_{WT}$ = 0.99 ± 0.04, $n$ = 4; $Emax_{Mecp2-/y}$ = 1.78 ± 0.21, n = 4; $p$ = 0.01, unpaired *t*-test; Fig. 1F). These data indicate higher neuronal excitability in the hippocampus of *Mecp2*$^{-/y}$ animals and that LTP impairment in *Mecp2*$^{-/y}$ animals is not due to a decrease in basal synaptic transmission efficiency.

### 3.2. BDNF and TrkB-FL receptor proteins are decreased in *Mecp2*$^{-/y}$ mice

Previous data suggest that MeCP2 acts both as a repressor and as an activator of gene expression (Chahrour et al., 2008). Given that the BDNF gene is under MeCP2 transcriptional regulation (Chen et al., 2003) attention has been directed to BDNF protein changes on RTT. Our results corroborate the previously described decrease in BDNF protein levels (for review see Li and Pozzo-Miller, 2014), both in the cerebral cortex and hippocampus ($HIP_{WT}$ = 100.0 ± 4.8%, $n$ = 8 *vs* $HIP_{Mecp2-/y}$ = 75.0 ± 7.2%, $n$ = 9, p = 0.01, unpaired t-test; $CTX_{WT}$ = 100.0 ± 10.9%, n = 8 *vs* $CTX_{Mecp2-/y}$ = 56.1 ± 3.7%, $n$ = 6, $p$ = 0.006, unpaired t-test; Fig. 1M;L).

However, the expression levels of TrkB-FL and its truncated isoform (TrkB-Tc), crucial players in BDNF mediated synaptic plasticity, had not yet been fully addressed. Therefore, we evaluated TrkB receptors levels in *Mecp2*$^{-/y}$ mice. As shown in Fig. 1G;H, TrkB-FL protein expression levels are decreased in both the cerebral cortex and the hippocampus of *Mecp2*$^{-/y}$ mice when compared to WT littermates ($HIP_{WT}$ = 100 ± 5.6%, $n$ = 13 *vs* $HIP_{Mecp2-/y}$ = 70.0 ± 9.4%, $n$ = 12; p = 0.01, unpaired *t*-test; $CTX_{WT}$ = 100.0 ± 5.3%, $n$ = 14 *vs* $CTX_{Mecp2-/y}$ = 66.2 ± 5.7%, $n$ = 13, $p$ = 0.0002, unpaired t-test; Fig. 1H). Regarding TrkB-Tc protein expression levels, no significant changes were detected ($HIP_{WT}$ = 100.0 ± 6.1%, n = 14 *vs* $HIP_{Mecp2-/y}$ = 94.5 ± 11.8%, n = 13, $p$ = 0.67, unpaired t-test; $CTX_{WT}$ = 100.0 ± 4.0%, n = 14 *vs* $CTX_{Mecp2-/y}$ = 83.7 ± 7.345%, n = 14, $p$ = 0.06, unpaired t-test Fig. 1I).

In addition, mRNA relative expression of both *TrkB-FL* and the most expressed TrkB-Tc (Luberg et al., 2010), *TrkB-T1,* were analysed by qPCR. As shown in Fig. 1J;K, no significant differences between WT and *Mecp2*$^{-/y}$ mice were detected ($TrkB\text{-}FL_{WT}$ = 0.12 ± 0.03, $n$ = 5 *vs* $TrkB\text{-}FL_{Mecp2-/y}$ = 0.18 ± 0.03, n = 5, $p$ = 0.22, unpaired *t*-test; $TrkB\text{-}T1_{WT}$ = 0.18 ± 0.03, n = 5 *vs* $TrkB\text{-}T1_{Mecp2-/y}$ = 0.2 ± 0.04, n = 5, $p$ = 0.39, unpaired t-test). Moreover, one *post-mortem* temporal cortex sample from a RTT patient was evaluated together with an aged-matched control. *TrkB-FL* mRNA expression in the temporal cortex of RTT patient showed a small increase (32.14%) when compared with the control (Fig. 1O). No apparent changes were observed regarding the mRNA expression levels of BDNF (Fig. 1N) and TrkB-Tc (Fig. 1P).

### 3.3. The adenosinergic modulation of synaptic transmission is compromised in *Mecp2*$^{-/y}$ mice

The lack of BDNF effect upon LTP could be explained by the decreased expression of TrkB-FL receptors in the hippocampus. However, since BDNF-induced facilitation of hippocampal LTP is tightly dependent on the activation of $A_{2A}R$ by endogenously generated adenosine (Fontinha et al., 2008), we next characterized the adenosinergic system in *Mecp2*$^{-/y}$ mice.

Brain extracts from *Mecp2*$^{-/y}$ mice exhibit lower ($p < 0.05$) adenosine amounts compared to WT animals in the cortex (WT = 35.49 ± 4.04 nmol, n = 8 *vs. Mecp2*$^{-/y}$ = 20.60 ± 2.91 nmol; n = 9, $p$-value = 0.009, Welch's *t*-test, Fig. 2A) and in the hippocampus (WT = 9.62 ± 0.99 nmol, n = 8 *vs. Mecp2*$^{-/y}$ = 5.55 ± 0.92 nmol; n = 8, $p$-value = 0.023, Welch's *t*-test, Fig. 2B), without any measurable changes in the levels of inosine. These results suggest that adenosine deficiency in RTT animals might not be related to increases in adenosine deaminase (ADA) activity. This prompted us to measure the amount of adenosine precursors (*e.g.* ATP and AMP) in the same samples. Brain extracts exhibit very small amounts of ATP, which levels did not differ among WT and *Mecp2*$^{-/y}$ mice both in the cortex (WT = 8.36 ± 1.77 nmol *vs. Mecp2*$^{-/y}$ = 6.34 ± 2.07 nmol; $n$ = 4; $p > 0.05$, Fig. 2A) and in the hippocampus (WT = 3.76 ± 1.77 nmol *vs. Mecp2*$^{-/y}$ = 2.19 ± 0.84 nmol; n = 4; $p > 0.05$, Fig. 2B). Contrariwise, higher AMP amounts compared to adenosine were extracted from the cortex (57.88 ± 3.57 nmol; n = 4) and hippocampus (30.28 ± 3.12 nmol; n = 4) of WT animals, but these levels also significantly ($p < 0.05$) decreased to 41.19 ± 1.30 nmol (n = 4) and 24.26 ± 2.64 nmol (n = 4) in the cortex and hippocampus of *Mecp2*$^{-/y}$ mice, respectively (Fig. 2A;B). The observed increase in the proportion of AMP *vis a vis* adenosine in cortical and hippocampal extracts of *Mecp2*$^{-/y}$ mice may indicate a decrease in 5′-nucleotidase activity, the enzyme responsible for AMP dephosphorylation into adenosine, and/or a higher competence of intracellular adenosine kinase (ADK) mediating phosphorylation of adenosine back to AMP. Next, we set to test the functional repercussions of having lower adenosine amounts in the hippocampus of *Mecp2*$^{-/y}$ mice compared to WT littermates. If our prediction is correct, facilitation (disinhibition) of hippocampal synaptic transmission produced by the selective $A_1R$ antagonist, DPCPX (Diogenes et al., 2014) should be less prominent in *Mecp2*$^{-/y}$ mice compared to WT animals. A supramaximal concentration of DPCPX (50 nM; $K_i$ value of 0.5 nM in the hippocampus (Sebastião et al., 1990)) was used to evaluate the effect of $A_1R$ blockage on basal synaptic transmission in hippocampal slices from *Mecp2*$^{-/y}$ mice and WT littermates. The magnitude of fEPSP slope in the presence of DPCPX (50 nM) was significantly higher in hippocampal slices from WT compared to those obtained from *Mecp2*$^{-/y}$ mice (WT = 45.3 ± 10.1%, n = 4, *vs. Mecp2*$^{-/y}$ = 23.4 ± 4.4%, $n$ = 10; $p$ = 0.0374, unpaired *t*-test; Fig. 2C).

Despite the reduction of the adenosine inhibitory tonus in hippocampal synaptic transmission in *Mecp2*$^{-/y}$ mice is in keeping with the observed low endogenous levels of the nucleoside in brain extracts (see above), $A_1R$ hypoactivity could also explain the results obtained. To sort this out, we tested the effect of the selective $A_1R$ agonist, CPA, at increasing concentrations (3, 10 and 30 nM). Exogenously added CPA concentration-dependently decreased fEPSP slope to a higher extent in *Mecp2*$^{-/y}$ mice compared to WT animals; this difference turn out to be significant ($p < 0.05$) at the highest concentration tested (30 nM) (WT = 31.4 ± 5.9%, $n$ = 7 *vs. Mecp2*$^{-/y}$ = 52.4 ± 6.530%, n = 7; p-value = 0.0345, unpaired t-test; Fig. 2D). These results (1) exclude the hypothesis that $A_1R$ are hypoactive in *Mecp2*$^{-/y}$ mice, (2) predict high expression rates of inhibitory $A_1R$ in the hippocampus of these animals, and (3) strengthens the theory that reduction of the inhibitory control of adenosine on hippocampal synaptic transmission in *Mecp2*$^{-/y}$ mice is mainly due to insufficient availability of the nucleoside at $A_1R$ sites. In the CNS, phosphorylation of adenosine leading to AMP formation by ADK is paramount to keep low intracellular levels of the nucleoside and, thus, it is considered the main driving force to take up adenosine from the extracellular milieu (Boison, 2013). Overexpression of ADK has been observed in astrocytes of epileptic brains of mice and humans (Aronica et al., 2011), which is consistent with the hypothesis that the pathophysiology of epilepsy involves lower endogenous adenosine levels and, thus, a deficient inhibition of synaptic transmission (Boison, 2013). Fig. 2E shows that the ADK protein level is not different in *Mecp2*$^{-/y}$ and WT mice, both in the hippocampus ($HIP_{WT}$ = 100.2 ± 8.1%, $n$ = 11 *vs.* $HIP_{Mecp2-/y}$ = 107.4 ± 11.24%, $n$ = 10, $p$ = 0.60, unpaired t-test) and in the cerebral cortex ($CTX_{WT}$ = 100.0 ± 4.3%, $n$ = 9 *vs.* $CTX_{Mecp2-/y}$ = 98.5 ± 5.8%, n = 10, $p$ = 0.84, unpaired *t*-test; Fig. 2E). It is, however, worth noting that Western Blot data reflects protein levels in whole tissue homogenates, not allowing the access to cell-specific protein contents at the synaptic level. Inhibition of

ADK is often used to reverse the nucleoside gradient across the plasma membrane leading to adenosine outflow *via* equilibrative nucleoside transporters (ENT) and its, subsequent, extracellular accumulation (Lee and Chao, 2001; Li et al., 2012). Here, we tested the effect of the ADK inhibitor, 5-iodotubercidin (5-ITU) (Pak et al., 1994), on basal hippocampal synaptic transmission. As shown in Fig. 2F, 5-ITU (100 nM) decreased fEPSP slope in hippocampal slices of both *Mecp2*$^{-/y}$ mice and WT littermates, but the effect of the ADK inhibitor had a higher ($P = 0.02$, unpaired *t*-test) inhibitory magnitude in WT (48.0 ± 6.6%, $n = 7$) compared to *Mecp2*$^{-/y}$ (25.2 ± 5.3%, $n = 6$) animals. Data show that inhibition of ADK could not fully overcome adenosine deficiency at the $A_1R$ level in the hippocampus of *Mecp2*$^{-/y}$ mice, thus indicating lower levels of endogenous adenosine.

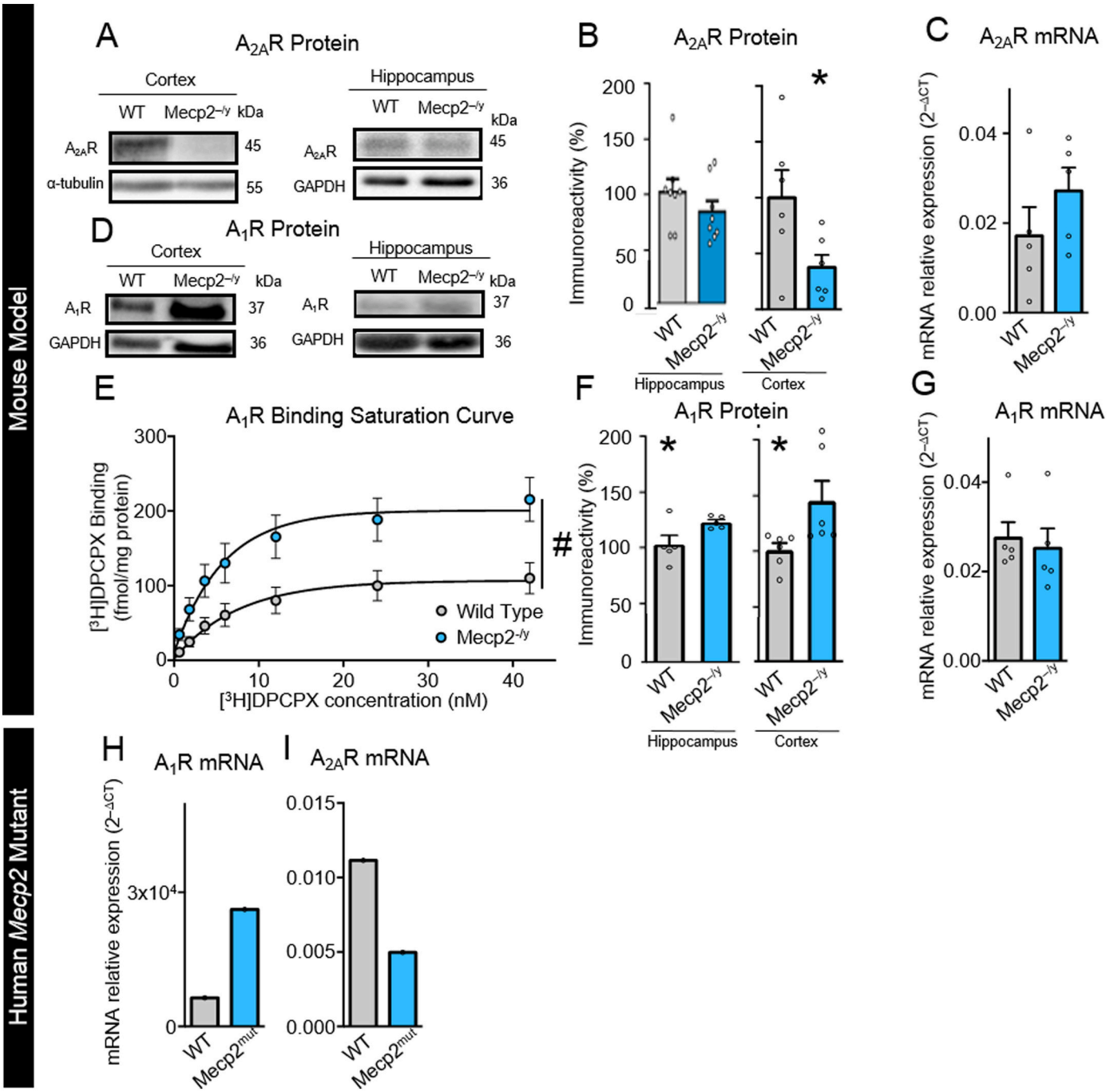


**Fig. 3.** $A_{2A}R$ protein expression is decreased and $A_1R$ is increased in Mecp2$^{-/y}$ mice: In A and B panels are shown the averaged $A_{2A}R$ receptors density while in D and F panels are shown the averaged $A_1R$ receptors density, all evaluated in hippocampal and cortical brain samples, respectively, by Western Blot analysis of WT (grey bar, $n_{hipA2AR} = 8$; $n_{ctxA2AR} = 6$; and $n_{hipA1R} = 5$; $n_{ctxA1R} = 6$) and Mecp2$^{-/y}$ (blue bars, $n_{ctxA2AR} = 6$; $n_{hipA2AR} = 8$ and $n_{ctxA1R} = 6$; $n_{hipA1R} = 5$) animals 6–10 weeks old. The results are represented in % of WT protein. In E are shown saturation isotherms for the binding of the selective $A_1R$ receptor antagonist [$^1$H]DPCPX to the cortical homogenates of WT (grey circles,n = 5) and Mecp2$^{-/y}$ (blue circles,$n = 6$) animals. In C and G are shown histograms representing the relative qPCR data showing mRNA levels of $A_{2A}R$ and $A_1R$, respectively, from cortical samples of WT (grey bar,n = 5) and Mecp2$^{-/y}$ mice (blue bar, n = 5). H and I histograms represent relative qPCR data showing mRNA levels of $A_1R$ and $A_{2A}R$, respectively, present in temporal cortex from a healthy control (grey bar,$n = 1$) and from a human RTT patient (blue bar,n = 1). All values are mean ± standard error of mean (SEM). *$p < 0.05$ (Student's *t*-test); #p < 0.05 (F test). (For interpretation of the references to colour in this figure legend, the reader is referred to the web version of this article.)

### 3.4. $A_{2A}R$ expression is decreased and $A_1R$ expression is increased in $Mecp2^{-/y}$ mice

To further understand how the adenosinergic system is disturbed in $Mecp2^{-/y}$ mice, we evaluated the $A_1R$ and $A_{2A}R$ expression at mRNA and protein levels. $A_{2A}R$ protein levels were assessed by Western Blot using an antibody validated against $A_{2A}R$ KO samples (supplementary Fig. 5A). Western Blot analysis of cortical and hippocampal homogenates show that $A_{2A}R$ protein amounts are significantly decreased in $Mecp2^{-/y}$ mice cortex compared to WT littermates and show a tendency for decreased $A_{2A}R$ protein levels in the hippocampus ($CTX_{WT}$ = 100.0% ± 24.8, $n = 6$ *vs* $CTX_{Mecp2-/y}$ = 37.5% ± 11.3, n = 6; $p = 0.04$, unpaired *t*-test; and $HIP_{WT}$ = 100.00 ± 11.78%, $n = 8$ and $HIP_{Mecp2-/y}$ = 82.19 ± 9.86%, n = 8; $p = 0.258$, unpaired t-test; Fig. 3A;B). Despite this, no significant differences were detected upon evaluating the $A_{2A}R$ mRNA relative expression in the two genotypes (WT = 0.017 ± 0.006, $n = 5$ *vs.* $Mecp2^{-/y}$ = 0.027 ± 0.005, n = 5, $p = 0.26$, unpaired t-test; Fig. 3C).

The existence of commercially available high affinity/high selectivity $A_1R$ ligands allowed us to perform receptor binding assays, which are frequently preferred (over Western Blot) for quantitative analysis of receptor expression whenever a considerable amount of tissue is available. Therefore, $A_1R$ were firstly evaluated by binding assays in cortical homogenates given the higher levels of protein content in this particular brain area. In Fig. 3E the saturation isotherms for the specific binding of the $A_1R$ antagonist, [$^3$H]DPCPX, show that this ligand binds more extensively to cortical brain homogenates of $Mecp2^{-/y}$ mice than to their WT littermates. The $B_{max}$ value obtained by nonlinear regression analysis, a measure of $A_1R$ expression levels, was significantly higher for $Mecp2^{-/y}$ mice (WT = 127.9 ± 17.1 fmol mg/protein, $n = 5$ *vs.* $Mecp2^{-/y}$ = 229.5 ± 22.1 fmol mg/protein, $n = 6$, $p = 0.007$, unpaired *t*-test). No significant differences in the $K_d$ values, a measure of receptor binding affinity, were found among the two genotypes (WT = 6.8 ± 2.7 nM, n = 5 *vs.* d $Mecp2^{-/y}$ = 4.3 ± 1.4 nM, n = 6, $p = 0.42$, unpaired t-test). By Western Blot technique similar data were obtained in cortex and hippocampus ($HIP_{WT}$ = 100.00 ± 7.88%, n = 5 *vs.* $HIP_{Mecp2-/y}$ = 119 ± 5.17,n = 5; $p = 0.049$, unpaired t-test; Fig. 3D;F and $CTX_{WT}$ = 100.0 ± 6.34, n = 6 *vs* $CTX_{Mecp2-/y}$ = 144 ± 17.81,n = 6; $p = 0.041$, unpaired t-test; Fig. 3D;F). Overall, data suggest that $A_1R$ expression levels are significantly increased in the cortex and hippocampus of $Mecp2^{-/y}$ animals compared to WT littermates. This difference may be owe to post-translational protein modifications, given to the fact that qPCR assays revealed no significant changes in cortical mRNA $A_1R$ gene transcripts (WT = 0.027 ± 0.004, n = 5 *vs.* $Mecp2^{-/y}$ = 0.025 ± 0.004, n = 5, $p = 0.7$, unpaired t-test; Fig. 3G). Interestingly, analyses of the temporal cortex from a RTT patient revealed a mRNA expression profile that is more consistent with the results obtained at the protein level in the mouse cortex, revealing an increase in $A_1R$ and a decrease in $A_{2A}R$ mRNA expression levels (Fig. 3H,I). The hippocampus of symptomatic heterozygous females (*Het*), where the phenotype is less severe, were also analysed (supplementary Fig. 5B). Similar changes in $A_1R$ and $A_{2A}R$ expression were detected in *Het* when compared to controls:1) significant decreased of $A_{2A}R$ protein levels in *Het* (WT = 100.00 ± 17.78%, n = 6 *vs. Het* = 52.47 ± 8.54%, n = 6, p = 0.04, unpaired *t*-test); 2) significant increase of $A_1R$ protein levels *Het* (WT = 100.00 ± 3.89%, n = 5 *vs. Het* = 116.60 ± 3.62%, n = 5, $p = 0.01$, unpaired t-test) supporting that adenosinergic system can be altered in several degrees of RTT severity.

### 3.5. Exogenous activation of $A_{2A}R$ restores BDNF-induced LTP facilitation in $Mecp2^{-/y}$ mice

The results reported above indicate that endogenous levels of adenosine and, thus, the nucleoside-mediated control of synaptic transmission are both deficient in the hippocampus of $Mecp2^{-/y}$ mice, along with a concomitant reduction of $A_{2A}R$ protein expression in this brain region. Therefore, we hypothesized that reduced adenosine $A_{2A}R$ tonus could also contribute to impairment of BDNF-mediated actions in RTT patients. Indeed, a strong body of evidence demonstrates that several BDNF actions rely on the activation of $A_{2A}R$ (Sebastião et al., 2011). Furthermore, this cross-talk was shown to be dynamic, for instance, during aging where the reduction of TrkB-FL receptor levels is accompanied by increases in $A_{2A}R$ levels (Diogenes et al., 2007). This prompted us to investigate whether activation of $A_{2A}R$ could be a feasible strategy to overcome BDNF signalling deficits in RTT patients, along with the reduced levels of this neurotrophin and to the partial loss of its TrkB-FL receptors. The selective $A_{2A}R$ agonist, CGS21680 (10 nM) (Jarvis et al., 1989) had no effect on the magnitude of LTP when it was applied alone to hippocampal slices of $Mecp2^{-/y}$ mice 1 h after LTP induction in the first pathway and at least 30 min before LTP induction in the second pathway; the magnitude of LTP in the absence ($LTP_{CTR}$ = 17,51 ± 6.70, $n = 7$) and presence

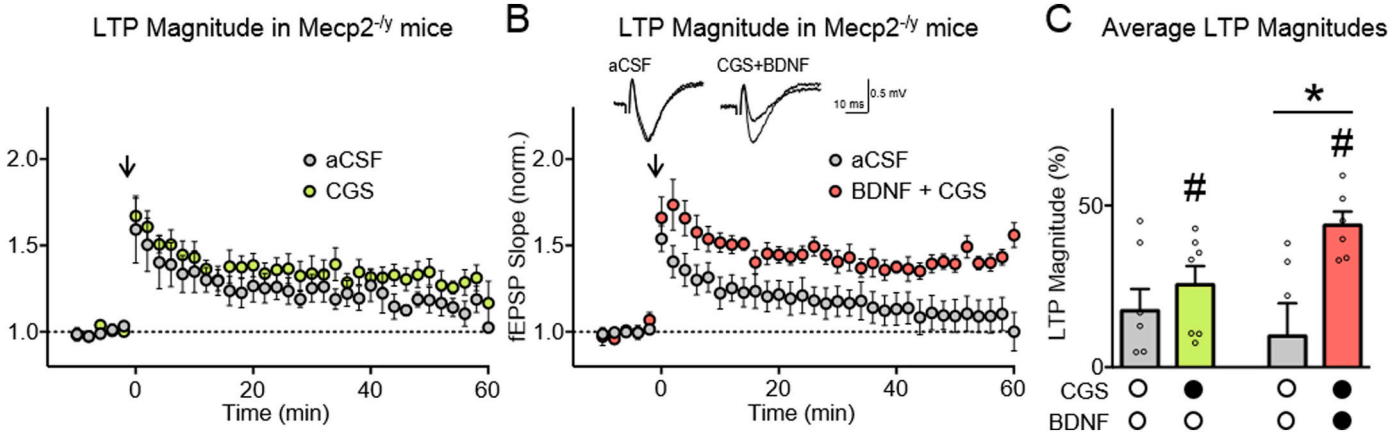


**Fig. 4.** Acute $A_{2A}R$ Activation restores BDNF effect upon LTP: A shows averaged time courses changes in field excitatory postsynaptic potential (fEPSP) slope induced by the θ-burst stimulation in the absence (grey circles) or in the presence (green circles) of the selective $A_{2A}$ receptor agonist, CGS21680 (10 nM) in hippocampal slices taken from Mecp2$^{-/y}$ mice (n = 7). CGS21680 (10 nM) was applied 60 min after the induction of LTP in the first pathway (grey circles) and at least 20 min before induction of LTP in the second pathway (green circles). B shows time courses changes of averaged fEPSP slopes in response to θ-burst stimulation in the absence (grey circles) or presence (red circles) of both CGS21680 (10 nM) and BDNF (20 ng/ml) in hippocampal slices taken from Mecp2$^{-/y}$ animals (n = 6). Representative traces from representative experiments are shown. Panel C depicts corresponding LTP magnitudes. All values are mean ± standard error of mean (SEM). *$p < 0.05$ (Student's t-test) #p < 0.05 (F test). (For interpretation of the references to colour in this figure legend, the reader is referred to the web version of this article.)

($LTP_{CGS}$ = 25.52 ± 5,79, n = 7) of CGS21680 did not significantly differ ($p$ = 0.25, paired $t$-test; Fig. 4A;C). However, in the presence of CGS21680, the LTP magnitude ($LTP_{CGS}$ = 25.52 ± 5,79, n = 7) is significantly different from the baseline (values obtained before the θ-burst; n = 7; p = 0.01, paired t-test, Fig. 4C), in contrast with what occurred in the absence of CGS21680. Next, we set to test whether activation of $A_{2A}R$ with CGS21680 could rehabilitate the facilitatory effect of BDNF on LTP when the neurotrophin was applied in a concentration (20 ng/ml) that was devoid of effect in hippocampal slices of *Mecp2*$^{-/y}$ mice (see Fig. 1D;E). In these experiments, LTP was induced in the first pathway in the absence of test drugs, then CGS21680 (10 nM) was applied 1 h after induction of the first LTP and BDNF (20 ng/ml) was applied 20 min after starting CGS21680 perfusion. The second pathway LTP was induced at least 30 min after starting BDNF application together with CGS21680. Co-application of BDNF (20 ng/ml) plus CGS21680 (10 nM) increased the magnitude of LTP in the hippocampus of *Mecp2*$^{-/y}$ mice ($LTP_{CTR}$ = 9.6 ± 10.2% *vs.* $LTP_{CGS+BDNF}$ = 43.9 ± 4.3%, $n$ = 6; $p$ = 0.048, paired t-test; Fig. 4B;C); the LTP magnitude attained under these conditions was fairly comparable to that obtained with BDNF alone in WT animals (see Fig. 1C;E). Data suggest that exogenous activation of $A_{2A}R$ with CGS21680 may rehabilitate BDNF signalling deficits observed in hippocampal LTP in *Mecp2*$^{-/y}$ mice, strengthening our theory that inadequacy of endogenous adenosine production plays a major role in synaptic transmission deficits in RTT patients.

## 4. Discussion

In the present work, we addressed an innovative strategy to potentiate BDNF effects in RTT through pharmacological modulation of adenosine receptors. While evaluating potential causes for the inability of exogenous BDNF to facilitate synaptic plasticity, we demonstrated that TrkB-FL receptors are decreased in the hippocampus and cerebral cortex of symptomatic *Mecp2*$^{-/y}$ mice and that the adenosinergic system is fully dysregulated, both at the receptor expression and functional levels. Pharmacological activation of $A_{2A}R$ was shown to recover the facilitatory action of BDNF upon synaptic plasticity.

BDNF is widely accepted as a neuroprotective molecule and, thus, BDNF-based therapies have been thoroughly explored to prevent neurodegeneration (Lu et al., 2013). Although RTT is not considered a neurodegenerative disorder, this interest has been extended to RTT were BDNF levels are known to be altered mainly in cortex, cerebellum and hippocampus (Abuhatzira et al., 2007; Chang et al., 2006; Li et al., 2012; Wang et al., 2006). A decrease of mRNA BDNF levels in *post-mortem* human brain samples of RTT patients has also been reported (Abuhatzira et al., 2007), though differences in BDNF protein levels in blood serum and cerebrospinal fluid from RTT human patients have been more difficult to show (Riikonen, 2003; Vanhala et al., 1998).

Much less was known about BDNF receptor signalling in RTT, and the existing data were conflicting. One study showed no differences in TrkB-FL mRNA levels between human embryonic stem cell derived from RTT neurons and controls (Li et al., 2013). Another study (Abuhatzira et al., 2007) showed that TrkB-FL mRNA expression levels are increased in a mouse model and in RTT human cortical brain samples, a change interpreted as a compensatory mechanism for the reduced BDNF protein levels detected in whole brain homogenates collected from newborn asymptomatic female mutant mice (Abuhatzira et al., 2007). By analysing the hippocampus and cortex of symptomatic male *Mecp2*$^{-/y}$ mice separately, we detected a significant decrease of BDNF protein levels and a tendency for an increase in mRNA levels of TrkB-FL and TrkB-Tc in both brain areas. A tendency for an increase in TrkB-FL mRNA in a *post-mortem* temporal cortex sample from a RTT patient was also observed. Importantly, none of the previous studies analysed in detail the protein levels of the different isoforms of the TrkB receptor, in particular whether putative alterations in the signalling form of the TrkB receptor, the TrkB-FL, were accompanied by changes in the truncated form of the receptor, the TrkB-Tc form, known to counteract TrkB signalling. Our data clearly shows that TrkB-FL protein levels are decreased in the hippocampus as well as in the cortex of symptomatic *Mecp2*$^{-/y}$ mice, without appreciable alterations in the truncated receptor protein levels. This may alter the way we should think about treatment, it is not only important to increase BDNF levels but it is also crucial to assure the presence of functional TrkB-FL receptors.

The idea that BDNF impairment could contribute to RTT pathophysiology was greatly reinforced by the finding that BDNF overexpression could partially ameliorate some of RTT symptoms in *Mecp2*$^{-/y}$ mice, including locomotor function, lifespan and the deficits on cortical electrophysiological activity (Chang et al., 2006). Overexpression of BDNF is, however, of very limited therapeutic use, if feasible at all. Other strategies are thus necessary to rescue BDNF function and to assure proper levels of TrkB-FL receptor. We aimed to potentiate BDNF actions through the major neuromodulator in the brain, adenosine. The reason to try this strategy is the previous evidence that, at least in healthy conditions, the synaptic actions of BDNF can be potentiated by activation of an adenosine receptor, the $A_{2A}R$ (Diógenes et al., 2004). $A_{2A}R$ activation induces transactivation of TrkB-FL (Lee and Chao, 2001), promotes translocation of TrkB receptors to lipid rafts (Assaife-Lopes et al., 2014; Sebastião et al., 2011) and regulates BDNF (Tebano et al., 2008) and TrkB-FL (Jerónimo-Santos et al., 2014) levels. Moreover, the effect of exogenous BDNF upon hippocampal synaptic transmission and LTP is dependent on a fully functional adenosinergic tonus *via* activation of $A_{2A}R$ (Diógenes et al., 2011, 2004; Fontinha et al., 2008). However, not all BDNF functions are adenosine dependent, which explain why some BDNF actions can be revealed even in the presence of and adenosinergic dysfunction, as shown in some previous papers (Chang et al., 2006). Dysfunction of adenosine signalling has been highlighted in several pathologies, such as sleep/arousal dysfunction, neurodegeneration, epilepsy, pain, neuronal maturation and central control of breathing (Gomes et al., 2011; Ribeiro et al., 2002), but has never been considered for RTT. This is surprising in light of the putative dual role of adenosine in this pathology: on the one hand, and as mentioned above, adenosine through $A_{2A}R$ influences BDNF actions; on the other hand, adenosine, mostly through $A_1R$, can control seizures in epileptic syndromes such as RTT (Boison, 2007; Sandau et al., 2016). Adenosine is an endogenous homeostatic regulator of network activity (Boison, 2012; Diogenes et al., 2014; Dunwiddie and Masino, 2001) and adenosine deficiency has been identified as a pathologic hallmark of the epileptic brain (Aronica et al., 2013). We found that *Mecp2*$^{-/y}$ mice displayed lower tonic inhibitory adenosinergic signalling in the hippocampus, as indicated by: 1) the lower disinhibition of excitatory synaptic transmission while blocking inhibitory $A_1R$; 2) the lower inhibition of synaptic transmission caused by an adenosine-releasing drug, as an ADK inhibitor; 3) lower levels of adenosine and AMP. This lower tonic adenosinergic inhibition is mostly likely due to the decreased levels of adenosine which might be related to lower expression and/or activity of 5′-nucleotidase resulting in the increased AMP/adenosine concentration ratio detected by us in hippocampus and cortex. On contrary, lower tonic adenosinergic inhibition cannot be accounted by lower ADK levels since *Mecp2*$^{-/y}$ mice had maintained ADK protein levels. The results obtained with the ADK inhibitor, which caused a lower inhibition of synaptic transmission in *Mecp2*$^{-/y}$ mice, are compatible with a lower adenosine gradient across the membrane, thus with decreased intracellular adenosine levels in *Mecp2*$^{-/y}$ mice, highly suggestive of dysregulated adenosine homeostasis. Adenosine levels are also dependent on ATP levels (Boison, 2015), therefore, we cannot exclude the potential role of dysregulated bioenergetics due to dysfunctional mitochondria in RTT. Although lower levels of ATP were already reported in the brain of *Mecp2*$^{-/y}$ mice (Saywell et al., 2006; Toloe et al., 2014), in the present work, we did not detected significant differences on the content of ATP when comparing hippocampus and cortex from WT and *Mecp2*$^{-/y}$ mice. Interestingly, studies performed in

organotypic hippocampal cultures have shown a downregulation on mitochondrial gene expression (Großer et al., 2012). Moreover, a quantitative decrease in electron transport chain units and reduced efficiency of glucose metabolism were found in RTT mouse models (De Filippis et al., 2015; Kriaucionis et al., 2006; Saywell et al., 2006). Also lower $A_1R$ receptor number or lower responsiveness of the $A_1R$ did not explain lower tonic adenosinergic inhibition because *Mecp2*$^{-/y}$ mice had enhanced $A_1R$ protein levels (as revealed by binding assays and western blot technique), and the response to an added $A_1R$ agonist was even higher in slices of *Mecp2*$^{-/y}$ mice. The mechanism underlying the overall increased levels of $A_1R$ remains unknown. However, we can speculate that this could be a compensatory mechanism to decreased levels of adenosine and to the overexcitability associated to this pathology. Indeed, in the brain of *Mecp2*$^{-/y}$ mice there is a tendency for hyperexcitability, associated to changes in basal inhibitory rhythms and pre- and postsynaptic defects in GABAergic synapses (Calfa et al., 2011). Low intracellular adenosine levels may favour DNA methylation and hence epileptogenesis (Williams-Karnesky et al., 2013). Consequently, adenosine augmentation therapies constitute an effective strategy to reduce seizures, even in cases refractory to conventional antiepileptic drugs (Boison, 2013, 2009).

In contrast with $A_1Rs$, the protein levels of $A_{2A}R$ were decreased in cortex of *Mecp2*$^{-/y}$ mice. The available receptors were nevertheless enough to respond to exogenous activation with a selective agonist, which was able to rescue the action of BDNF on synaptic plasticity (LTP). This further reinforces the hypothesis that adenosine augmentation therapies may be a particularly useful strategy in a disease that simultaneously involves low BDNF signalling and low capability of endogenous adenosine to act as an endogenous anticonvulsant. As it occurred with the mRNA of the $A_1R$, the mRNA expression level of $A_{2A}R$ was not significantly affected in *Mecp2*$^{-/y}$ mice. The discrepancy between mRNA and protein expression levels could be attributed to several posttranscriptional mechanisms such as deregulation of AKT/mTOR in RTT, an important signalling pathway for protein synthesis and which it is under the regulatory influence of MeCP2 (Li et al., 2013). Intriguingly, it was possible to detect changes in the mRNA levels of both $A_1R$ and $A_{2A}R$ in one *post-mortem* human brain sample from an RTT patient, and the changes detected closely mimicked the changes detected at the protein level in *Mecp2*$^{-/y}$ mice. The advanced disease stage of the donor child and the inherent differences between mice models and humans may explain the discrepancy regarding mRNA expression levels. Nevertheless, we should acknowledge the limitations of this analysis: samples from only one mRNA RTT patient were available, and it was thus not possible to access variability in different subjects. Considering the high influence of the heterozygosity in this syndrome, we conducted some preliminary experiences to know if the adenosinergic system is also changed in a milder phenotype such as the heterozygotic mice female. The results showed similar changes found in the hippocampus from *Mecp2*$^{-/y}$: decreased protein levels of $A_{2A}R$ and increased protein levels in $A_1R$. Moreover, the alterations detected in mRNA expression levels of $A_{2A}R$ and $A_1R$ support a similar deregulation in adenosinergic system in the sample from a RTT patient with a different genotype (*MeCP2* mutation - R255X). These results strongly support the hypothesis that the adenosinergic system is changed in multiple phenotypes of RTT. Taken together, the results show a decrease on endogenous adenosine levels and a consequent impairment on adenosinergic signalling in RTT. This deregulation could hamper BDNF signalling and may account for epileptogenesis and decrease seizure control, therefore opening new avenues for RTT therapy: adenosine augmentation therapies (AAT). AAT have been already explored in other pathologies, such as in epilepsy (Boison, 2009). Interestingly, RTT patients present some disturbances related with deregulation on adenosinergic system such dysfunction in sleep/arousal, neuronal maturation, central control of breathing and epilepsy, (Gomes et al., 2011; Ribeiro et al., 2002). Our findings showing alterations in adenosine system in RTT strongly point towards a possible contribution of adenosine system in RTT pathophysiology. To potentiate BDNF signalling it could be enough to target only $A_{2A}R$. However, our results shed light into the relevance of using AATs instead of direct $A_{2A}R$ activation. IndeeTs would target the two high affinity adenosine receptors and trigger their activation to promote: 1) the rescue of BDNF effects, through $A_{2A}R$; 2) the control of hyperexcitability through $A_1R$. In addition, it was already shown that adenosine plays an important role in epileptogenesis through an epigenetic action by DNA methylation, which inhibits epileptogenesis (Williams-Karnesky et al., 2013). As previous discussed, AAT could be achieved by genetic approaches and cell-therapy strategies (as discussed in Boison, 2009).

Subsequent work should elucidate whether MeCP2 directly affects the expression of enzymes that regulate adenosine and adenosine receptor expression. It is possible that changes in receptor levels result of homeostatic mechanisms (Sandau et al., 2016) attempting to preserve inhibitory ADO synaptic actions by increasing inhibitory $A_1R$ and decreasing excitatory $A_{2A}R$ expression levels. However, in the case of RTT where BDNF expression and signalling is impaired, the decrease of $A_{2A}R$ further aggravates the disease. Importantly, as we herein show, in spite of the reduction of $A_{2A}R$ expression and the decreased levels of endogenous adenosine, the pharmacological activation of $A_{2A}R$ could efficiently rescue BDNF effects upon synaptic plasticity.

## 5. Conclusion

In conclusion, we found that BDNF actions upon hippocampal LTP are impaired in RTT. This dysfunction can be explained by the changes in TrkB receptor levels and in adenosinergic neuromodulation. Importantly, by understanding that the adenosinergic system is compromised in RTT, we can now advance that deregulation of BDNF signalling can also be due to impairment of endogenous $A_{2A}R$ activation. This study thus sets the stage for new adenosine-based pharmacological therapeutic strategies for RTT, for which disease modifying drugs are still lacking.

Supplementary data to this article can be found online at https://doi.org/10.1016/j.nbd.2020.105043.

## Ethics approval

Studies in *post-mortem* brain of *MECP2* patients were included in the project “Therapeutic approaches in Rett syndrome” funded by “Mi Princesa Rett”, a Spanish Patient Association. This study was approved by the Ethics Committee of HSJD and parents provided informed written consent.

## Funding

The work was supported by a joint research grant awarded to TMR from Fundação Calouste Gulbenkian and FMUL (20130002/PEC/BG); Fundação para a Ciência e Tecnologia (FCT, AdoRett – LISBOA-01-0145-FEDER-031929/2017 and FCT SFRH/BD/118238/2016 granted to CML); Universidade de Lisboa (grant awarded by CML BD2015); the Association Française du Syndrome de Rett; Program “Educação pela Ciência” Bolsas CHLN/FMUL – GAPIC (Project No. 20190017); Twinning action (SynaNet) from the EU H2020 Programme; and the UID/BIM/50005/2019, project financed by the FCT/Ministério da Ciência, Tecnologia e Ensino Superior (MCTES), through the Fundos do Orçamento de Estado. The work performed at ICBAS/MedInUP by PCS and TMC was partially supported by FCT (FEDER funding, project UID/BIM/4308/2019 and UIDP/04308/2020).

## Declaration of Competing Interest

The authors declare that they have no competing interests.

## Acknowledgments

We are indebted to “Mi Princesa Rett” that is a Spanish Patietns' Association that contributed in the study funding. We are indebted to the “Biobank de Hospital infantil Sant Joan de Déu per la Investigació” integrated in the Spanish Biobank Networkof ISCIII for the sample and the data procurement. We acknowledge “Associação Nacional de Pais e Amigos Rett” (ANPAR). We would like to thank to Joana E. Coelho, PhD, and Luísa V. Lopes, PhD, from Instituto de Medicina Molecular João Lobo Antunes, for providing the $A_{2A}R$ KO mouse cortex sample.

## References

Abuhatzira, L., Makedonski, K., Kaufman, Y., Razin, A., Shemer, R., 2007. MeCP2 deficiency in the brain decreases BDNF levels by REST/CoREST-mediated repression and increases TRKB production. Epigenetics 2, 214–222. https://doi.org/10.4161/epi.2.4.5212.

Amir, R.E., Van den Veyver, I.B., Wan, M., Tran, C.Q., Francke, U., Zoghbi, H.Y., 1999. Rett syndrome is caused by mutations in X-linked MECP2, encoding methyl-CpG-binding protein 2. Nat. Genet. 23, 185–188. https://doi.org/10.1038/13810.

Anderson, W.W., Collingridge, G.L., 2001. The LTP Program: A data acquisition program for on-line analysis of long-term potentiation and other synaptic events. J. Neurosci. Methods 108, 71–83. https://doi.org/10.1016/S0165-0270(01)00374-0.

Aronica, E., Zurolo, E., Iyer, A., De Groot, M. De, Anink, J., 2011. Upregulation of adenosine kinase in astrocytes in experimental and human temporal lobe epilepsy. Epilepsia 52, 1645–1655. https://doi.org/10.1111/j.1528-1167.2011.03115.x. Upregulation.

Aronica, E., Sandau, U.S., Iyer, A., Boison, D., 2013. Glial adenosine kinase - A neuropathological marker of the epileptic brain. Neurochem. Int. 63, 688–695. https://doi.org/10.1016/j.neuint.2013.01.028.

Asaka, Y., Jugloff, D.G.M., Zhang, L., Eubanks, J.H., Fitzsimonds, R.M., 2006. Hippocampal synaptic plasticity is impaired in the Mecp2-null mouse model of Rett syndrome. Neurobiol. Dis. 21, 217–227. https://doi.org/10.1016/j.nbd.2005.07.005.

Assaife-Lopes, N., Sousa, V.C., Pereira, D.B., Ribeiro, J.A., Sebastião, A.M., 2014. Regulation of TrkB receptor translocation to lipid rafts by adenosine A(2A) receptors and its functional implications for BDNF-induced regulation of synaptic plasticity. Purinergic Signal 10, 251–267. https://doi.org/10.1007/s11302-013-9389-9.

Batalha, V.L., Ferreira, D.G., Coelho, J.E., Valadas, J.S., Gomes, R., Temido-Ferreira, M., Shmidt, T., Baqi, Y., Buée, L., Müller, C.E., Hamdane, M., Outeiro, T.F., Bader, M., Meijsing, S.H., Sadri-Vakili, G., Blum, D., Lopes, L.V., 2016. The caffeine-binding adenosine A2A receptor induces age-like HPA-axis dysfunction by targeting glucocorticoid receptor function. Sci. Rep. 6, 31493. https://doi.org/10.1038/srep31493.

Bedogni, F., Rossi, R.L., Galli, F., Cobolli Gigli, C., Gandaglia, A., Kilstrup-Nielsen, C., Landsberger, N., 2014. Rett syndrome and the urge of novel approaches to study MeCP2 functions and mechanisms of action. Neurosci. Biobehav. Rev. 46, 187–201. https://doi.org/10.1016/j.neubiorev.2014.01.011.

Binder, D.K., Scharfman, H.E., 2004. Brain-derived neurotrophic factor. Growth Factors 22, 123–131. https://doi.org/10.1016/j.bbi.2008.05.010.

Boison, D., 2007. Adenosine as a modulator of brain activity. Drug News Perspect. 20, 607. https://doi.org/10.1358/dnp.2007.20.10.1181353.

Boison, D., 2009. Adenosine augmentation therapies (AATs) for epilepsy: Prospect of cell and gene therapies. Epilepsy Res. 85, 131–141. https://doi.org/10.1016/j.eplepsyres.2009.03.019.

Boison, D., 2012. Adenosine dysfunction in epilepsy. Glia 29, 997–1003. https://doi.org/10.1016/j.biotechadv.2011.08.021.Secreted.

Boison, D., 2013. Adenosine kinase: exploitation for therapeutic gain. Pharmacol. Rev. 65, 906–943. https://doi.org/10.1124/pr.112.006361.

Boison, D., 2015. Adenosinergic signaling in epilepsy. Neuropharmacology. https://doi.org/10.1016/j.neuropharm.2015.08.046.

Calfa, G., Hablitz, J.J., Pozzo-Miller, L., 2011. Network hyperexcitability in hippocampal slices from Mecp2 mutant mice revealed by voltage-sensitive dye imaging. J. Neurophysiol. 105, 1768–1784. https://doi.org/10.1152/jn.00800.2010.

Chahrour, M., Zoghbi, H.Y., 2007. The story of Rett syndrome: From clinic to neurobiology. Neuron 56, 422–437. https://doi.org/10.1016/j.neuron.2007.10.001.

Chahrour, M., Jung, S.Y., Shaw, C., Zhou, X., Wong, S.T.C., Qin, J., Zoghbi, H.Y., 2008. MeCP2, a key contributor to neurological disease, activates and represses transcription. Science 320, 1224–1229. https://doi.org/10.1126/science.1153252.

Chang, Q., Khare, G., Dani, V., Nelson, S., Jaenisch, R., 2006. The disease progression of Mecp2 mutant mice is affected by the level of BDNF expression. Neuron 49, 341–348. https://doi.org/10.1016/j.neuron.2005.12.027.

Chen, W.G., Chang, Q., Lin, Y., Meissner, A., West, A.E., Griffith, E.C., Jaenisch, R., Greenberg, M.E., 2003. Derepression of BDNF transcription involves calcium-dependent phosphorylation of MeCP2. Science 302, 885–889. https://doi.org/10.1126/science.1086446.

Chen, J.F., Sonsalla, P.K., Pedata, F., Melani, A., Domenici, M.R., Popoli, P., Geiger, J., Lopes, L.V., de Mendonça, A., 2007. Adenosine A2A receptors and brain injury: Broad spectrum of neuroprotection, multifaceted actions and “fine tuning” modulation. Prog. Neurobiol. 83, 310–331. https://doi.org/10.1016/j.pneurobio.2007.09.002.

De Filippis, B., Valenti, D., De Bari, L., De Rasmo, D., Musto, M., Fabbri, A., Ricceri, L., Fiorentini, C., Laviola, G., Vacca, R.A., 2015. Mitochondrial free radical overproduction due to respiratory chain impairment in the brain of a mouse model of Rett syndrome: Protective effect of CNF1. Free Radic. Biol. Med. 83, 167–177. https://doi.org/10.1016/j.freeradbiomed.2015.02.014.

Deng, V., Matagne, V., Banine, F., Frerking, M., Ohliger, P., Budden, S., Pevsner, J., Dissen, G.a., Sherman, L.S., Ojeda, S.R., 2007. FXYD1 is an MeCP2 target gene overexpressed in the brains of Rett syndrome patients and Mecp2-null mice. Hum. Mol. Genet. 16, 640–650. https://doi.org/10.1093/hmg/ddm007.

Diógenes, M.J., Fernandes, C.C., Sebastião, A.M., Ribeiro, J.A., 2004. Activation of adenosine A2A receptor facilitates brain-derived neurotrophic factor modulation of synaptic transmission in hippocampal slices. J. Neurosci. 24, 2905–2913. https://doi.org/10.1523/JNEUROSCI.4454-03.2004.

Diogenes, M. j, Assaife-Lopes, N., Pinto-Duarte, A., Ribeiro, J.A., Sebastião, A.M., 2007. Influence of age on bdnf modulation of hippocampal synaptic transmission: Interplay with adenosine a2a receptors. Hippocampus 000, 1–3. https://doi.org/10.1002/hipo.

Diógenes, M.J., Costenla, A.R., Lopes, L.V., Jerónimo-Santos, A., Sousa, V.C., Fontinha, B.M., Ribeiro, J. a, Sebastião, A.M., 2011. Enhancement of LTP in aged rats is dependent on endogenous BDNF. Neuropsychopharmacology 36, 1823–1836. https://doi.org/10.1038/npp.2011.64.

Diogenes, M.J., Dias, R.B., Rombo, D.M., Vicente Miranda, H., Maiolino, F., Guerreiro, P., Nasstrom, T., Franquelim, H.G., Oliveira, L.M.a., Castanho, M.a.R.B., Lannfelt, L., Bergstrom, J., Ingelsson, M., Quintas, a., Sebastiao, a.M., Lopes, L.V., Outeiro, T.F., 2012. Extracellular alpha-synuclein oligomers modulate synaptic transmission and impair LTP via NMDA-receptor activation. J. Neurosci. 32, 11750–11762. https://doi.org/10.1523/JNEUROSCI.0234-12.2012.

Diogenes, M.J., Neves-Tome, R., Fucile, S., Martinello, K., Scianni, M., Theofilas, P., Lopatar, J., Ribeiro, J.A., Maggi, L., Frenguelli, B.G., Limatola, C., Boison, D., Sebastiao, A.M., 2014. Homeostatic control of synaptic activity by endogenous adenosine is mediated by adenosine kinase. Cereb. Cortex 24, 67–80. https://doi.org/10.1093/cercor/bhs284.

Dunwiddie, T.V., Masino, S.A., 2001. The role and regulation of adenosine in the central nervous system. Annu. Rev. Neurosci. 24, 31–55. https://doi.org/10.1146/annurev.neuro.24.1.31.

Eide, F.F., 1996. Naturally occuring truncated trkb receptors have dominant inhibitory effects on brain-derived neurotrophic factor signaling. J. Neurosci. 16, 3123–3129. https://doi.org/10.1055/s-0029-1237430.Imprinting.

Figurov, A., Pozzo-Miller, L.D., Olafsson, P., Wang, T., Lu, B., 1996. Regulation of synaptic responses to high-frequency stimulation and LTP by neurotrophins in the hippocampus. Nature 381, 706–709. https://doi.org/10.1038/381706a0.

Fontinha, B.M., Diógenes, M.J., Ribeiro, J.a., Sebastião, a.M., 2008. Enhancement of long-term potentiation by brain-derived neurotrophic factor requires adenosine A2A receptor activation by endogenous adenosine. Neuropharmacology 54, 924–933. https://doi.org/10.1016/j.neuropharm.2008.01.011.

Gomes, C.V., Kaster, M.P., Tomé, A.R., Agostinho, P.M., Cunha, R. a, 2011. Adenosine receptors and brain diseases: Neuroprotection and neurodegeneration. Biochim. Biophys. Acta 1808, 1380–1399. https://doi.org/10.1016/j.bbamem.2010.12.001.

Großer, E., Hirt, U., Janc, O.A., Menzfeld, C., Fischer, M., Kempkes, B., Vogelgesang, S., Manzke, T.U., Opitz, L., Salinas-Riester, G., Müller, M., 2012. Oxidative burden and mitochondrial dysfunction in a mouse model of Rett syndrome. Neurobiol. Dis. 48, 102–114. https://doi.org/10.1016/j.nbd.2012.06.007.

Guy, J., Hendrich, B., Holmes, M., Martin, J.E., Bird, a, 2001. A mouse Mecp2-null mutation causes neurological symptoms that mimic Rett syndrome. Nat. Genet. 27, 322–326. https://doi.org/10.1038/85899.

Guy, J., Gan, J., Selfridge, J., Cobb, S., Bird, A., 2007. Reversal of neurological defects in a mouse model of Rett syndrome. Science 315, 1143–1147. https://doi.org/10.1126/science.1138389.

Huang, E.J., Reichardt, L.F., 2003. Trk receptors: Roles in neuronal signal transduction. Annu. Rev. Biochem. 72, 609–642. https://doi.org/10.1146/annurev.biochem.72.121801.161629.

Jackson, E.K., Kotermanski, S.E., Menshikova, E.V., Dubey, R.K., Jackson, T.C., Kochanek, P.M., 2017. Adenosine production by brain cells. J. Neurochem. 141, 676–693. https://doi.org/10.1111/jnc.14018.

Jarvis, M.F., Schulz, R., Hutchison, A.J., Do, U.H., Sills, M.A., Williams, M., 1989. [3H]CGS 21680, a selective A2 adenosine receptor agonist directly labels A2 receptors in rat brain. J. Pharmacol. Exp. Ther. 251, 888–893.

Jerónimo-Santos, A., Batalha, V.L., Müller, C.E., Baqi, Y., Sebastião, A.M., Lopes, L.V., Diógenes, M.J., 2014. Impact of in vivo chronic blockade of adenosine A2A receptors on the BDNF-mediated facilitation of LTP. Neuropharmacology 83, 99–106. https://doi.org/10.1016/j.neuropharm.2014.04.006.

Karpova, N.N., Lindholm, J.S.O., Kulesskaya, N., Onishchenko, N., Vahter, M., Popova, D., Ceccatelli, S., Castrén, E., 2014. TrkB overexpression in mice buffers against memory deficits and depression-like behavior but not all anxiety- and stress-related symptoms induced by developmental exposure to methylmercury. Front. Behav. Neurosci. 8, 315. https://doi.org/10.3389/fnbeh.2014.00315.

Kriaucionis, S., Paterson, A., Curtis, J., Guy, J., MacLeod, N., Bird, A., 2006. Gene expression analysis exposes mitochondrial abnormalities in a mouse model of Rett syndrome. Mol. Cell. Biol. 26, 5033–5042. https://doi.org/10.1128/MCB.01665-05.

Lee, F.S., Chao, M.V., 2001. Activation of Trk neurotrophin receptors in the absence of neurotrophins. Proc. Natl. Acad. Sci. U. S. A. 98, 3555–3560. https://doi.org/10.1073/pnas.061020198.

Lewis, J.D., Meehan, R.R., Henzel, W.J., Maurer-Fogy, I., Jeppesen, P., Klein, F., Bird, a, 1992. Purification, sequence, and cellular localization of a novel chromosomal protein that binds to methylated DNA. Cell 69, 905–914. https://doi.org/10.1016/0092-8674(92)90610-O.

Li, W., Pozzo-Miller, L., 2014. BDNF deregulation in Rett syndrome. Neuropharmacology 76, 737–746. https://doi.org/10.1016/j.neuropharm.2013.03.024.

Li, W., Calfa, G., Larimore, J., Pozzo-Miller, L., 2012. Activity-dependent BDNF release and TRPC signaling is impaired in hippocampal neurons of Mecp2 mutant mice. Proc. Natl. Acad. Sci. 109, 17087–17092. https://doi.org/10.1073/pnas.1205271109.

Li, Y., Wang, H., Muffat, J., Cheng, a W., Orlando, D. a, Loven, J., Kwok, S.M., Feldman, D. a, Bateup, H.S., Gao, Q., Hockemeyer, D., Mitalipova, M., Lewis, C. a, Vander Heiden, M.G., Sur, M., Young, R. a, Jaenisch, R., 2013. Global transcriptional and translational repression in human-embryonic-stem-cell-derived Rett syndrome neurons. Cell Stem Cell 13, 446–458. https://doi.org/10.1016/j.stem.2013.09.001.

Liyanage, V.R.B., Rastegar, M., 2014. Rett syndrome and MeCP2. NeuroMolecular Med. 16, 231–264. https://doi.org/10.1007/s12017-014-8295-9.

Lu, B., Nagappan, G., Guan, X., Nathan, P.J., Wren, P., 2013. BDNF-based synaptic repair as a disease-modifying strategy for neurodegenerative diseases. Nat. Rev. Neurosci. 14, 401–416. https://doi.org/10.1038/nrn3505.

Luberg, K., Wong, J., Weickert, C.S., Timmusk, T., 2010. Human TrkB gene: Novel alternative transcripts, protein isoforms and expression pattern in the prefrontal cerebral cortex during postnatal development. J. Neurochem. 113, 952–964. https://doi.org/10.1111/j.1471-4159.2010.06662.x.

Minichiello, L., Korte, M., Wolfer, D., Kühn, R., Unsicker, K., Cestari, V., Rossi-Arnaud, C., Lipp, H.P., Bonhoeffer, T., Klein, R., 1999. Essential role for TrkB receptors in hippocampus-mediated learning. Neuron 24, 401–414.

Moretti, P., Levenson, J.M., Battaglia, F., Atkinson, R., Teague, R., Antalffy, B., Armstrong, D., Arancio, O., Sweatt, J.D., Zoghbi, H.Y., 2006. Learning and memory and synaptic plasticity are impaired in a mouse model of Rett syndrome. J. Neurosci. 26, 319–327. https://doi.org/10.1523/JNEUROSCI.2623-05.2006.

Neul, J.L., Lane, J.B., Lee, H.-S., Geerts, S., Barrish, J.O., Annese, F., Baggett, L.M., Barnes, K., Skinner, S. a, Motil, K.J., Glaze, D.G., Kaufmann, W.E., Percy, A.K., 2014. Developmental delay in Rett syndrome: Data from the natural history study. J. Neurodev. Disord. 6, 20. https://doi.org/10.1186/1866-1955-6-20.

Nicolini, C., Ahn, Y., Michalski, B., Rho, J.M., Fahnestock, M., 2015. Decreased mTOR signaling pathway in human idiopathic autism and in rats exposed to valproic acid. Acta Neuropathol. Commun. 3, 3. https://doi.org/10.1186/s40478-015-0184-4.

Pak, M.A., Haas, H.L., Decking, U.K., Schrader, J., 1994. Inhibition of adenosine kinase increases endogenous adenosine and depresses neuronal activity in hippocampal slices. Neuropharmacology 33, 1049–1053.

Poduslo, J.F., Curran, G.L., 1996. Permeability at the blood-brain and blood-nerve barriers of the neurotrophic factors: NGF, CNTF, NT-3, BDNF. Mol. Brain Res. 36, 280–286. https://doi.org/10.1016/0169-328X(95)00250-V.

Rei, N., Rombo, D.M., Ferreira, M.F., Baqi, Y., Müller, C.E., Ribeiro, J.A., Sebastião, A.M., Vaz, S.H., 2020. Hippocampal synaptic dysfunction in the SOD1G93A mouse model of amyotrophic lateral sclerosis: Reversal by adenosine A2AR blockade. Neuropharmacology 171. https://doi.org/10.1016/j.neuropharm.2020.108106.

Ribeiro, J.A., Sebastião, A.M., de Mendonça, A., 2002. Adenosine receptors in the nervous system: Pathophysiological implications. Prog. Neurobiol. 68, 377–392. https://doi.org/10.1016/S0301-0082(02)00155-7.

Riikonen, R., 2003. Neurotrophic factors in the pathogenesis of Rett syndrome. J. Child Neurol. 18, 693–697. https://doi.org/10.1177/08830738030180101101.

Robinson, L., Guy, J., McKay, L., Brockett, E., Spike, R.C., Selfridge, J., De Sousa, D., Merusi, C., Riedel, G., Bird, A., Cobb, S.R., 2012. Morphological and functional reversal of phenotypes in a mouse model of Rett syndrome. Brain 135, 2699–2710. https://doi.org/10.1093/brain/aws096.

Rombo, D.M., Dias, R.B., Duarte, S.T., Ribeiro, J. a, Lamsa, K.P., Sebastião, A.M., 2014. Adenosine A1 receptor suppresses tonic GABAA receptor currents in hippocampal pyramidal cells and in a defined subpopulation of interneurons. Cereb. Cortex 1–15. https://doi.org/10.1093/cercor/bhu288.

Rose, C.R., Blum, R., Pichler, B., Lepier, A., Kafitz, K.W., Konnerth, A., 2003. Truncated TrkB-T1 mediates neurotrophin-evoked calcium signalling in glia cells. Nature 426, 74–78. https://doi.org/10.1038/nature01983.

Sandau, U.S., Colino-Oliveira, M., Jones, A., Saleumvong, B., Coffman, S.Q., Liu, L., Miranda-Lourenço, C., Palminha, C., Batalha, V.L., Xu, Y., Huo, Y., Diógenes, M.J., Sebastião, A.M., Boison, D., 2016. Adenosine kinase deficiency in the brain results in maladaptive synaptic plasticity. J. Neurosci. 36.

Saywell, V., Viola, A., Confort-Gouny, S., Le Fur, Y., Villard, L., Cozzone, P.J., 2006. Brain magnetic resonance study of Mecp2 deletion effects on anatomy and metabolism. Biochem. Biophys. Res. Commun. 340, 776–783. https://doi.org/10.1016/j.bbrc.2005.12.080.

Schmittgen, T.D., Livak, K.J., 2008. Analyzing real-time PCR data by the comparative C(T) method. Nat. Protoc. 3, 1101–1108. https://doi.org/10.1038/nprot.2008.73.

Sebastião, a M., Ribeiro, J. a, 2009. Tuning and fine-tuning of synapses with adenosine. Curr. Neuropharmacol. 7, 180–194. https://doi.org/10.2174/157015909789152128.

Sebastião, A.M., Stone, T.W., Ribeiro, J.A., 1990. The inhibitory adenosine receptor at the neuromuscular junction and hippocampus of the rat: Antagonism by 1,3,8-substituted xanthines. Br. J. Pharmacol. 101, 453–459.

Sebastião, A.M., Assaife-Lopes, N., Diógenes, M.J., Vaz, S.H., Ribeiro, J. a, 2011. Modulation of brain-derived neurotrophic factor (BDNF) actions in the nervous system by adenosine A(2A) receptors and the role of lipid rafts. Biochim. Biophys. Acta 1808, 1340–1349. https://doi.org/10.1016/j.bbamem.2010.06.028.

Silva, I., Costa, A.F., Moreira, S., Ferreirinha, F., Magalhães-Cardoso, M.T., Calejo, I., Silva-Ramos, M., Correia-de-Sá, P., 2017. Inhibition of cholinergic neurotransmission by $\beta_3$ -adrenoceptors depends on adenosine release and $A_1$ -receptor activation in human and rat urinary bladders. Am. J. Physiol. Physiol. 313, F388–F403. https://doi.org/10.1152/ajprenal.00392.2016.

Silva, I., Magalhães-Cardoso, M.T., Ferreirinha, F., Moreira, S., Costa, A.F., Silva, D., Vieira, C., Silva-Ramos, M., Correia-de-Sá, P., 2020. $\beta_3$ Adrenoceptor-induced cholinergic inhibition in human and rat urinary bladders involves the exchange protein directly activated by cyclic AMP 1 favoring adenosine release. Br. J. Pharmacol. 14921. https://doi.org/10.1111/bph.14921.

Tebano, M.T., Martire, a., Potenza, R.L., Grò, C., Pepponi, R., Armida, M., Domenici, M.R., Schwarzschild, M.a., Chen, J.F., Popoli, P., 2008. Adenosine A2A receptors are required for normal BDNF levels and BDNF-induced potentiation of synaptic transmission in the mouse hippocampus. J. Neurochem. 104, 279–286. https://doi.org/10.1111/j.1471-4159.2007.05046.x.

Toloe, J., Mollajew, R., Kügler, S., Mironov, S.L., 2014. Metabolic differences in hippocampal "Rett" neurons revealed by ATP imaging. Mol. Cell. Neurosci. 59, 47–56. https://doi.org/10.1016/j.mcn.2013.12.008.

Tsvyetlynska, N.A., Hill, R.H., Grillner, S., n.d. Role of AMPA Receptor Desensitization and the Side Effects of a DMSO Vehicle on Reticulospinal EPSPs and Locomotor Activity. https://doi.org/10.1152/jn.00201.2005.

Vanhala, R., Korhonen, L., Mikelsaar, M., Lindholm, D., Riikonen, R., 1998. Neurotrophic factors in cerebrospinal fluid and serum of patients with Rett syndrome. J. Child Neurol. 13, 429–433. https://doi.org/10.1177/088307389801300903.

Vieira, C., Ferreirinha, F., Magalhães-Cardoso, M.T., Silva, I., Marques, P., Correia-de-Sá, P., 2017. Post-inflammatory ileitis induces non-neuronal purinergic signaling adjustments of cholinergic neurotransmission in the myenteric plexus. Front. Pharmacol. 8, 811. https://doi.org/10.3389/fphar.2017.00811.

Wang, H., Chan, S., Ogier, M., Hellard, D., Wang, Q., Smith, C., Katz, D.M., 2006. Dysregulation of brain-derived neurotrophic factor expression and neurosecretory function in Mecp2 null mice. J. Neurosci. 26, 10911–10915. https://doi.org/10.1523/JNEUROSCI.1810-06.2006.

Williams-Karnesky, R.L., Sandau, U.S., Lusardi, T.A., Lytle, N.K., Farrell, J.M., Pritchard, E.M., Kaplan, D.L., Boison, D., 2013. Epigenetic changes induced by adenosine augmentation therapy prevent epileptogenesis. J. Clin. Invest. 123, 3552–3563. https://doi.org/10.1172/JCI65636.